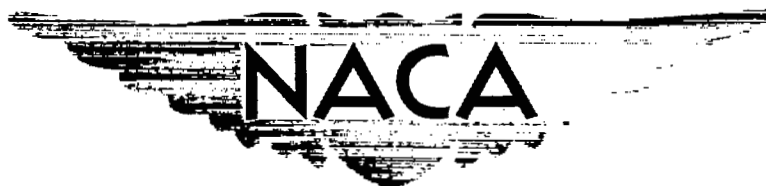


CONFIDENTIAL

Copy 6  
RM L54C05

NACA RM L54C05



# RESEARCH MEMORANDUM

EFFECT ON THE LOW-SPEED AERODYNAMIC CHARACTERISTICS OF A  
49° SWEEPBACK WING HAVING AN ASPECT RATIO OF 3.78 OF  
BLOWING AIR OVER THE TRAILING-EDGE FLAP AND AILERON

By Edward F. Whittle, Jr., and Stanley Lipson

Langley Aeronautical Laboratory  
Langley Field, Va.

CLASSIFICATION CANCELLED

Authority *NASA Res. Lab.* Date *10-18-56*

*4-10-108*

By *NB 11-2-56* See

CLASSIFIED DOCUMENT

This material contains information affecting the National Defense of the United States within the meaning of the espionage laws, Title 18, U.S.C., Secs. 793 and 794, the transmission or revelation of which in any manner to an unauthorized person is prohibited by law.

**NATIONAL ADVISORY COMMITTEE  
FOR AERONAUTICS**

WASHINGTON

April 23, 1954

**LIBRARY COPY**

APR 28 1954

LANGLEY AERONAUTICAL LABORATORY  
LIBRARY, NACA  
LANGLEY FIELD, VIRGINIA

CONFIDENTIAL

## NATIONAL ADVISORY COMMITTEE FOR AERONAUTICS

## RESEARCH MEMORANDUM

EFFECT ON THE LOW-SPEED AERODYNAMIC CHARACTERISTICS OF A  
49° SWEEPBACK WING HAVING AN ASPECT RATIO OF 3.78 OF  
BLOWING AIR OVER THE TRAILING-EDGE FLAP AND AILERON

By Edward F. Whittle, Jr., and Stanley Lipson

## SUMMARY


An investigation has been conducted in the Langley full-scale tunnel to determine the effects on the aerodynamic characteristics of a 49.1° sweptback wing of blowing a high-energy stream of air over a trailing-edge flap and an aileron. The wing configuration was investigated with and without a slat and fences. The wing had an aspect ratio of 3.78, a taper ratio of 0.59, and NACA 65A006 airfoil sections parallel to the plane of symmetry. The tests were conducted at Reynolds numbers of  $2.9 \times 10^6$ ,  $4.4 \times 10^6$ , and  $6.1 \times 10^6$  corresponding to Mach numbers of 0.05, 0.07, and 0.10, respectively.

The results show that significant increases in lift coefficient and an improvement in aileron effectiveness may be obtained by the blowing method of boundary-layer control on a plain flap and aileron.

## INTRODUCTION

The reduced lift capabilities of conventional high-lift devices when applied to sweptback-wing aircraft constitute a severe low-speed performance problem. Means for improving the maximum lift capabilities of the sweptback wing are being investigated extensively by the National Advisory Committee for Aeronautics.

One method now receiving attention is that of blowing a high-velocity (that is, a velocity that is high relative to the magnitude of the free-stream velocity) jet of air over the trailing-edge flap with the primary aim of adding sufficient energy locally as to either eliminate or at least reduce the tendency for flow separation over the flap. This method of boundary-layer control appears to be especially attractive for application to jet-powered aircraft inasmuch as a high-pressure source of air would be readily available.



Early German two-dimensional tests, such as those reported in reference 1, indicated that large increases in lift coefficient could be obtained by blowing a high-energy stream of air over a trailing-edge flap. A French investigation (ref. 2) extended the blowing technique to application on a moderately sweptback wing ( $31.3^\circ$ ) in conjunction with suction at about the midchord of the wing. In these French tests, approximately the rear 45 percent of the wing chord was divided into two chordwise segments which could be deflected. As in the case of the earlier two-dimensional tests, the results appeared to be very promising; however, analysis of the effects due to blowing is necessarily limited since only a few tests were conducted with blowing alone over the trailing-edge flap (zero suction at the midchord of the wing).

In view of the possibility, then, of increasing wing lift by means of blowing over the trailing-edge flap, the method has been extended to the case of a highly swept, thin wing. Tests have been conducted in the Langley full-scale tunnel on a semispan  $49.1^\circ$  sweptback wing having NACA 65A006 airfoil sections, an aspect ratio of 3.78, and a taper ratio of 0.59. Preliminary tests were conducted with a low-capacity blower and are presented in reference 3. Because of the very low pressure rise and quantity of flow of the blower, no significant results were obtained. The investigation reported herein is a continuation of the full-scale-tunnel blowing tests but with a multistage, large-flow-capacity blower. The tests were made with and without a slat and fences installed and with and without blowing over a trailing-edge flap or trailing-edge flap and aileron. Tests were also made to determine the rolling effectiveness produced by blowing air over the aileron. In addition, some chordwise pressure distributions were obtained at the midspan of the trailing-edge flap in order to study the load change that occurred as a result of the blowing method of boundary-layer control.

The tests were made at Reynolds numbers of  $2.9 \times 10^6$ ,  $4.4 \times 10^6$ , and  $6.1 \times 10^6$  corresponding to Mach numbers of 0.05, 0.07, and 0.10, respectively.

#### COEFFICIENTS AND SYMBOLS

The data are referred to the wind axes with the origin at the quarter-chord point of the mean aerodynamic chord. The data have been reduced to standard NACA nondimensional coefficients which, together with the symbols, are defined as follows:

$C_L$  lift coefficient,  $\frac{\text{Twice model lift}}{q_\infty S}$

- $\Delta C_{L\alpha=0}$  value of  $C_L$  at  $\alpha = 0^\circ$  for a given configuration minus value of  $C_L$  at  $\alpha = 0^\circ$  for basic wing
- $C_{L_{\max}}$  maximum lift coefficient
- $\Delta C_{L_{\max}}$  value of  $C_{L_{\max}}$  for a given configuration minus value of  $C_{L_{\max}}$  for basic wing
- $\Delta C_{L_B}$  value of  $C_L$  for a given configuration with blowing at a given angle of attack minus value of  $C_L$  for the same configuration without blowing at the same angle of attack
- $C_D$  drag coefficient,  $\frac{\text{Twice model drag}}{q_0 S}$
- $C_m$  pitching-moment coefficient about quarter-chord point of mean aerodynamic chord,  $\frac{\text{Twice model pitching moment}}{q_0 S \bar{c}}$
- $C_l$  rolling-moment coefficient,  $\frac{\text{Rolling moment}}{q_0 S b}$
- $C_p$  duct pressure coefficient,  $\frac{H_d - p_0}{q_0}$
- $C_Q$  flow coefficient,  $\frac{Q}{V_0 S'}$
- $C_\mu$  momentum coefficient in plane perpendicular to blowing slot,  $Q_0 j V_j / q_0 S'$
- $c_{c_f}$  flap section chord-force coefficient,  $\frac{t'_{f_{\max}}}{c'_f} \int_{-1}^1 P \, d\left(\frac{t'_f}{t'_{f_{\max}}}\right)$
- $c_{n_f}$  flap section normal-force coefficient,  $\int_0^1 P_R \, d\left(\frac{x'_f}{c'_f}\right)$

- $c_{hf}$  flap section hinge-moment coefficient about leading edge of flap,  $\int_0^1 P_R \frac{x'_f}{c'_f} d\left(\frac{x'_f}{c'_f}\right)$
- $P$  wing surface pressure coefficient,  $\frac{P - P_0}{q_0}$
- $P_R$  resultant wing surface pressure coefficient,  $P_{upper} - P_{lower}$
- $b$  twice span of semispan wing model, ft
- $c$  local wing chord measured parallel to plane of symmetry, ft
- $c'$  local wing chord measured perpendicular to 0.50c' line (midchord line of wing in unswept position), ft (see fig. 1)
- $\bar{c}$  mean aerodynamic chord,  $\frac{2}{S} \int_0^{b/2} c^2 dy$ , ft
- $c_{av}$  average chord of wing area  $S'$  affected by the blowing air, measured in streamwise direction, ft
- $c'_f$  local trailing-edge flap chord measured perpendicular to 0.50c' line (see fig. 1), ft
- $c'_s$  local slat chord measured perpendicular to 0.50c' line (see fig. 1), ft
- $s$  blowing-slot gap, ft
- $t'_f$  flap section thickness at various chordwise stations on chord perpendicular to 0.50c' line, ft
- $t'_{f_{max}}$  maximum flap section thickness on chord perpendicular to 0.50c' line, ft
- $x'_f$  chordwise distance from leading edge of  $c'_f$ , ft
- $\left(\frac{x'_f}{c'_f}\right)_{cp}$  chordwise location from leading edge of  $c'_f$  of section center of pressure

$y_{cp}$	spanwise location of wing center of pressure, measured from and perpendicular to plane of symmetry, $2y/b$
$p$	local static pressure, lb/sq ft
$H_d$	duct total pressure, lb/sq ft
$p_o$	free-stream static pressure, lb/sq ft
$q_o$	free-stream dynamic pressure, lb/sq ft
$S$	twice area of semispan wing model, sq ft
$S'$	twice area of semispan wing model affected by blowing air, sq ft
$R$	Reynolds number, $\frac{\rho_o V_o \bar{c}}{\mu}$
$V_o$	free-stream velocity, ft/sec
$V_j$	jet velocity of blowing air perpendicular to slot exit, ft/sec
$\rho_o$	mass density of free-stream air, slugs/cu ft
$\rho_j$	mass density of blowing air, slugs/cu ft
$\mu$	coefficient of viscosity of air, slugs/ft-sec
$Q$	twice quantity of blowing air, cu ft/sec
$\alpha$	angle of attack, deg
$\delta_f$	flap deflection (relative to wing-chord line) measured perpendicular to $0.50c'$ line, deg
$\delta_a$	aileron deflection (relative to wing-chord line) measured perpendicular to $0.50c'$ line, deg

## MODEL AND APPARATUS

Model.— The geometric characteristics and principal dimensions of the semispan wing are given in figure 1 and details of the slat, fences, and flap are given in figure 2. A photograph of the wing mounted on the reflection plane in the Langley full-scale tunnel is given as figure 3 and a description of the reflection plane is given in reference 4. The wing has  $49.1^\circ$  of sweepback at the leading edge, an aspect ratio of 3.78, a taper ratio of 0.59, and no geometric twist or dihedral. The airfoil sections parallel to the plane of symmetry are NACA 65A006 sections and the wing tip is half of a body of revolution based on the same airfoil section ordinates.

The high-lift and stall-control devices used (see figs. 1 and 2) are: a 0.266c' inboard trailing-edge flap having a span of  $0.469b/2$ ; a 0.266c' flap-type aileron, which only could be deflected down, located immediately outboard of the flap and having a span of  $0.234b/2$ ; a 0.15c' leading-edge slat having a span of  $0.500b/2$ , measured inboard from the wing tip; and chordwise fences having a height of 0.06c and located at spanwise stations, measured outboard from the plane of symmetry, of  $0.6b/2$  or  $0.6b/2$  and  $0.8b/2$ .

The nose and upper surface of the slat have the ordinates of the wing airfoil. The slat is not an integral part of the wing but is mounted directly onto the unmodified leading edge of the basic wing with the slat brackets aligned normal to the leading edge of the wing. The fences are made of 1/4-inch plywood and are mounted parallel to the plane of symmetry.

Just ahead of the trailing-edge flap and aileron is a slot (fig. 2) which opens into the upper portion of the gap between the airfoil and the flap and aileron. The slot is used for blowing a high-energy stream of air over the upper surface of the flap and aileron. The wing area affected by blowing over the flap is 76.4 square feet and the wing area affected by blowing over the aileron and flap is 108.0 square feet.

At the midspan of the flap a thin strip of belt pressure tubing was glued to the surface of the flap perpendicular to the 0.50c' line (see fig. 1) at one spanwise station so that flap chordwise pressure distributions could be obtained for several of the configurations tested.

Blower-ducting apparatus.— A modified compressor of a jet engine, driven through a 2.6 to 1 ratio gearbox by two 200-horsepower electric motors in tandem, was used as the pumping source for the boundary-layer-control air. The compressor was modified by removing three of the six stages in order to reduce the pressure rise and horsepower requirements for driving the compressor at high flow quantities. The three remaining

stages of the modified compressor produced a pressure rise of 1.2 at the maximum compressor speed tested. A calibrated entrance bell, installed at the compressor inlet, was used to determine the mass flow of air. A shielded thermocouple and a shielded total-pressure tube were used to obtain the temperature and pressure of the boundary-layer-control air at the wing root. These temperature and pressure measurements were used in conjunction with the known flow weight in order to determine the flow quantity of the boundary-layer-control air.

The blower is connected to the blowing slot ahead of the flap and aileron by a duct inside the wing which extends through the reflection plane at the wing root. A mercury seal was used beneath the reflection plane between the wing duct and the stationary blower duct in order to prevent transmission of forces from the stationary duct to the wind-tunnel scale system. The blowing-slot gap could be varied by manually adjusting a spanwise series of throttling plates. As a result of springing of the wing upper surface at the blowing slot, the blowing-slot gap, with the blower operating at 9,600 rpm, was about 0.004c when the flap was deflected and about 0.003c when the flap and aileron were deflected. A rake of shielded total-pressure tubes was employed to check the resulting velocity distribution along the blowing slot. The velocity of the air exiting from and perpendicular to the blowing slot ahead of the flap (aileron blowing slot sealed) varied from 415 ft/sec at the outboard end of the flap to 450 ft/sec at the inboard end of the flap to give an integrated average velocity of 425 ft/sec. The velocity of the air exiting from and perpendicular to the blowing slot ahead of the aileron and flap varied from 388 ft/sec at the outboard end of the aileron to 448 ft/sec at the inboard end of the flap to give an integrated average velocity of 404 ft/sec. The largest variation occurred over about the inboard 30 percent of the flap span, with the highest velocity at the very inboard end of the flap.

#### TESTS, CORRECTIONS, AND DATA PRESENTATION

Tests.— An index of the test conditions and configurations tested is given in table I. Data were obtained through an angle-of-attack range from approximately  $-4^{\circ}$  to  $31^{\circ}$ . Force measurements were made to determine the lift, drag, pitching moment, and spanwise center-of-pressure variation of the basic wing and the wing with various combinations of the high-lift and stall-control devices without and with blowing a high-energy stream of air over the flap or flap and aileron. The rolling-moment characteristics of the aileron were determined with the trailing-edge flap neutral and deflected, and with and without blowing. With blowing, the flow coefficient  $C_Q$  was varied by varying either blower rotational speed or tunnel velocity.



Chordwise pressure distributions were obtained on the trailing-edge flap at the midspan station for several test conditions. Flow studies, using woolen tufts attached to the upper surface of the wing, were made for several of the wing configurations. The tests were made at Reynolds numbers of  $2.9 \times 10^6$ ,  $4.4 \times 10^6$ , and  $6.1 \times 10^6$  corresponding to Mach numbers of 0.05, 0.07, and 0.10, respectively.

Corrections.— The data have been corrected for airstream misalignment, blocking effects, and jet-boundary effects. The jet-boundary corrections follow the method outlined in reference 5 for semispan wings. The rolling-moment correction for the effects of the reflection plane, as discussed in reference 4, was obtained from unpublished results based on the methods of references 6 and 7.

Presentation of drag data.— In comparing the drag characteristics of a wing employing boundary-layer control by blowing with the drag characteristics of a wing not employing boundary-layer control, account must be taken of the following three increments:

(1) Aerodynamic drag of the wing-flap arrangement (including the thrust effect of the blowing air).

(2) Air intake and duct drag due to ducting the free-stream air to the boundary-layer control pump.

(3) Drag equivalent of the pump horsepower needed to produce the required quantity of boundary-layer-control air and pressure rise at the blowing slot.

The drag coefficients presented herein represent only the first drag increment mentioned above. The drag data are presented in this manner because increments (2) and (3) would vary with any specific airplane-duct and blowing-slot arrangement under consideration. Drag increment (3) may be found from  $C_p C_q$ . Since the latter two drag increments have been neglected, the aerodynamic drag data presented often have a negative value at low angles of attack and high values of  $C_q$  inasmuch as the thrust due to blowing air over the flap is larger than the drag of the wing configuration.

## RESULTS AND DISCUSSION

### Presentation of Results

The basic data are presented in figures 4 to 17, and figures 18 to 21 present a summary of the more significant results. Figure 22 illustrates the variation of  $C_\mu$  obtained with  $C_q$  for the subject wing.

A wide range of values of the momentum coefficient  $C_\mu$  could be obtained during this investigation only by using large values of  $C_Q$  and blowing-slot gap, since the compressor and power available for blowing limited the available pressure rise and thus restricted this investigation to testing at moderate values of blowing-slot exiting velocities. Even though the maximum values of  $C_Q$  may be unrealistically high, it is felt that the effects obtained are indicative of those that would be obtained at similar values of  $C_\mu$  produced by combining high blowing-slot exiting velocities with low flow rates typical of bleed systems having high pressure and small mass flow that are currently adapted from turbojet-engine installations. Since  $\frac{C_\mu}{2C_Q} = \frac{V_j}{V_o}$ , it may be seen that for any given combination of  $C_\mu$  and  $C_Q$  the ratio  $V_j/V_o$  is fixed. For this fixed ratio of  $V_j/V_o$ , then, there is some value of  $V_o$  which, if exceeded, will require a supersonic  $V_j$ . The most critical  $C_Q - C_\mu$  combination tested herein was the case of  $C_Q = 0.042$  and  $C_\mu = 0.68$  for which condition the limiting value of  $V_o$  would be a Mach number of 0.12. Therefore, for landing or take-off speeds above a Mach number of 0.12, a supersonic blowing jet would be required to obtain this aforementioned  $C_Q - C_\mu$  combination. It is of interest to note that, for the subject wing, the required blowing-slot pressure coefficient  $C_p$  could be accurately estimated by the method of reference 8 which indicates that  $C_p$  for a blowing arrangement of the type tested may be considered as being approximately equal to  $(V_j/V_o)^2$ . The values of  $C_p$  computed by this simple relationship are 16, 34, and 66 as compared to measured values of 15, 31, and 70 for the case of the flap deflected  $53^\circ$  and corresponding values of  $C_Q$  of 0.02, 0.03, and 0.04.

#### Lift Characteristics

A summary of the variation of  $\Delta C_{L_{\alpha=0}}$  and  $\Delta C_{L_{\max}}$  with flow coefficient  $C_Q$  and momentum coefficient  $C_\mu$  is presented in figures 20 and 21, respectively.

With the slat and fences installed, the maximum-lift gains obtained for the 0.47b/2 flap deflected  $53^\circ$  and the 0.70b/2 flap (that is, flap plus aileron) deflected  $53^\circ$  are as follows:

Flap span, b/2	$\Delta C_{L\alpha=0}$	$\Delta C_{L_{max}}$	$C_Q$	$C_\mu$
0.47	0.39 .94	0.12 .63	0 .042	0 .68
.70	.46 1.14	.16 .68	0 .030	0 .56

The increase in  $C_L$  obtained by applying suction on a flap may be attributed to the increased circulation around the wing associated with alleviation of separation on the flap. When applying suction to a flap, then, the maximum increase in  $C_L$  is limited to that associated with obtaining the theoretical flap effectiveness. By blowing a high-energy stream of air over a flap, however, the maximum increase in  $C_L$  can be greater than the increase associated with obtaining the theoretical flap effectiveness. This additional increase in  $C_L$  is probably associated with (1) for  $\alpha > 0^\circ$ , a lift component due to the thrust of the ejected air and (2) an increase in circulation around the wing due to a flow condition simulating a physical extension of the flap chord and resulting from the momentum of the ejected air.

It was of interest to determine whether the theoretical lift increment for a 0.47b/2 flap deflected  $53^\circ$  ( $44^\circ$  in the streamwise direction) was realized by blowing air over the upper surface of the trailing-edge flap. It was calculated, by means of reference 9, that the theoretical lift increment was 0.70, and this lift increment was obtained during the tests for  $\alpha = 0^\circ$  at  $C_\mu = 0.25$  ( $C_Q = 0.025$ ).

The results presented in figure 21 show that, at a given value of  $C_\mu$ , increasing the flap deflection from  $45^\circ$  to  $53^\circ$  produced a small increase in  $\Delta C_{L\alpha=0}$  but actually slightly reduced  $\Delta C_{L_{max}}$  in the  $C_\mu$  range tested. From a study of certain pitching-moment data, as discussed in the section on "Pitching-Moment Characteristics," it is believed that, for the higher values of  $C_Q$  and flap angle the blowing air was not properly impinging on the upper surface of the flap. It may well be, then, that for a flap deflection of  $53^\circ$  a more efficient slot arrangement would not only have resulted in a higher  $C_{L_{max}}$  than was obtained

at  $\delta_f = 45^\circ$ , but correspondingly, the theoretical lift increment of 0.70 could have been obtained at a value of  $C_\mu$  lower than 0.25.

For the  $53^\circ$  flap deflection, the installation of a slat and fences had no effect on  $\Delta C_{L_{\alpha=0}}$ . The increase in  $\Delta C_{L_{\max}}$ , especially at the higher values of  $C_\mu$ , results from delaying the separation over the outboard sections to a higher value of  $C_L$ . These results indicate that in order to realize the full benefits of a blowing system for improving lift, stall-control devices must be used to prevent early stalling over the critically affected portion of the wing.

By deflecting the aileron in combination with the 0.47b/2 flap, a continuous flap span of 0.70b/2 could be obtained. A comparison of the relative effectiveness of the two different flap arrangements with blowing can be made either on the basis of equal  $C_Q$  or equal air quantity  $Q$ . When compared on the basis of equal  $C_Q$ ,  $\Delta C_{L_{\alpha=0}}$  and  $\Delta C_{L_{\max}}$  are larger for the larger flap span than for the smaller flap span for the range of  $C_Q$  tested (fig. 20). It should be noted that, on the basis of equal compressor air quantities, values of  $C_Q$  of approximately 0.03 ( $C_\mu = 0.35$ ) and 0.04 ( $C_\mu = 0.61$ ) for the flap-deflected configuration correspond to values of  $C_Q$  of about 0.02 ( $C_\mu = 0.21$ ) and 0.03 ( $C_\mu = 0.46$ ), respectively, for the configuration with the flap plus aileron deflected. Deflecting the aileron, then, reduced the quantity being ejected over the flap and probably reduced the local circulation on the flapped portion of the wing. However, the increased lift on the outboard part of the wing containing the aileron was such that at low and moderate angles of attack the overall wing lift was greater than that obtained by blowing the total air flow over the flap alone. A comparison of figures 11 and 12 and figures 20 and 21 indicates that, for a given air flow,  $C_{L_{\alpha=0}}$  was increased about 20 percent to 30 percent by deflecting the aileron. Beyond an angle of attack of about  $7^\circ$ , the wing lift-curve slope for the 0.70b/2 flap configuration was reduced as compared to the case of blowing over the 0.47b/2 flap. This difference appears to be a result of a more rapid reduction in flap load at the moderate angles of attack for the 0.70b/2 flap configuration due to its lower  $C_Q$  (see section on "Pitching-Moment Characteristics"). The rougher flow obtained at the higher angles of attack over the deflected flap and aileron for the 0.70b/2 flap arrangement, as compared to the 0.47b/2 flap configuration, is evident in figure 13. The net result, then, was that deflecting the aileron to  $53^\circ$ , without increasing  $Q$ , and employing it as a high-lift device produced only a small increase in  $C_{L_{\max}}$ .

## Pitching-Moment Characteristics

The particular combination of sweep, aspect ratio, and airfoil thickness of the wing used in this investigation resulted in a severe longitudinal-stability problem. Blowing increased the magnitude of the lift coefficient at which the initial unstable pitching-moment break occurred but also tended to increase the severity of this instability. In general, longitudinal instability occurs at a lift coefficient about 0.2 to 0.3 less than  $C_{L_{max}}$ . Note, for example, the results presented in figure 11 for the 0.47b/2 flap deflected  $53^\circ$ , slat and fences installed. For values of  $C_Q$  of 0.022, 0.029, and 0.042, an unstable pitching-moment break occurs at values of  $C_L$  of 1.03, 1.14, and 1.34, respectively. For their respective flow coefficients, these lift coefficients correspond to a wing angle of attack of about  $7^\circ$ . Part of this instability is associated with unloading of the flap at the higher lift coefficients. Figure 15(b) indicates a large reduction in flap normal-force coefficient at the higher lift coefficients for the  $C_Q \approx 0.03$  flow condition.

In view of some previous investigations on swept wings (for example, ref. 10) it is probable that, once unseparated flow over the flap has been established, further improvements, and possibly alleviation, of the wing pitch-up near  $C_{L_{max}}$  could have been obtained by a more extensive exploration of a combination of leading-edge devices and trailing-edge flaps. The major effort of this initial investigation, however, was directed toward determining the general influence of a boundary-layer-control system of the type proposed herein on the lift of the wing.

The pitching-moment data of figures 7, 11, and 12 show that a positive trim shift results from increased blowing effort; this result is contrary to the negative trim shift expected for a progressive increase in flap loading. The unpublished results obtained for a wing having the same leading-edge sweep, but of a somewhat lower aspect ratio (3.2), showed a similar effect due to nonadherence of the blowing jet stream to the upper surface of the flap. In the case of this lower aspect ratio wing, employing a guide vane in the blowing slot to redirect the jet stream, and thus improving the jet-stream adherence to the flap, produced an additional trim shift of -0.08 as compared to the case of poor jet-stream adherence. It is surmised, then, that for the subject wing of the present investigation, nonadherence of the flow over the flap probably occurred at values of  $C_Q$  above about 0.03 for the  $\delta_f = 53^\circ$  configuration (see fig. 7) and at values of  $C_Q$  of about 0.02 for the  $\delta_f = 60^\circ$  condition (see fig. 5). Although this lack of flow adherence appears to have markedly reduced the flap loading for the condition where  $\delta_f = 53^\circ$  and  $C_Q \approx 0.03$ , as evidenced by the stability result, it does not seem

to have been severe enough to induce separation over the flap (see flow studies in fig. 13 and flap section pressure distribution in fig. 14); this suggests that the section chordwise center of pressure or the span loading itself was also critically sensitive to this particular flap system under the influence of a blowing jet.

Comparison with a conventional high-lift flap.- Reference 11 reports the results of tests conducted with the same wing used for this investigation but employing a Fowler type flap having the same span as the plain flap tested herein. Although it is recognized that both the Fowler flap arrangements of reference 11 and the blowing configuration investigated herein may not represent "optimum" arrangements, it is believed that a comparison of the results of these two investigations will be indicative of the gains to be realized on a wing of large leading-edge sweep.

In judging the comparative effectiveness of these two flap systems, it should be stated that the Fowler flap had a chord of  $0.20c'$  as compared to  $0.266c'$  for the flap configuration herein. With a  $0.50b/2$  slat installed and fences located at  $0.60b/2$  and  $0.80b/2$ , the Fowler flap produced lift increments  $\Delta C_{L_{\alpha=0}}$  and  $\Delta C_{L_{max}}$  of 0.42 and 0.24, respectively, at a deflection of  $45^\circ$  as compared with 0.75 and 0.42, respectively, for the blowing flap at  $\delta_f = 53^\circ$  and  $C_Q = 0.029$ .

From the stability standpoint, the negative trim shifts obtained with some of the blowing configurations (see, for example, fig. 12) were of the same order or less than those produced by the Fowler flap.

Investigations of various slotted flap arrangements on highly swept wings (such as those discussed in ref. 12) have shown the highest effective flap deflection angle to be about  $45^\circ$ . However, as demonstrated in this investigation, a flap system utilizing some mechanical means of boundary-layer control makes it possible to employ effectively greater flap deflections.

#### Flap Pressure Distribution

Typical results of the pressure-distribution tests that were made at a single station located at the midspan of the flap are presented in figure 14. At an angle of attack of  $15.2^\circ$ , without blowing, the flap was stalled, but with blowing at  $C_Q \approx 0.03$  the flap was not stalled. The flap section chord-force coefficient, normal-force coefficient, chordwise center-of-pressure location, and hinge-moment coefficient are shown in figure 15 as a function of  $C_L$ . Without blowing, increasing the flap deflection from  $30^\circ$  to  $53^\circ$  increased the normal-force coefficient, moved the chordwise center-of-pressure rearward, and increased the hinge-moment coefficient but had little effect on the chord-force coefficient. With

blowing at  $C_Q \approx 0.03$  the chord-force coefficient was increased in the thrust direction, the normal-force coefficient was increased, the chordwise center of pressure was shifted forward, and the hinge-moment coefficient was increased. With blowing, increasing the flap deflection from  $30^\circ$  to  $53^\circ$  had a larger effect on the chord-force coefficient than occurred in the case without blowing.

### Rolling-Moment Characteristics

All aileron tests were made with a  $0.5b/2$  slat installed and fences located at  $0.6b/2$  and  $0.8b/2$  spanwise stations and only positive deflections of the aileron. The results of the aileron tests, with and without blowing, are presented in figures 16 and 17. Except as noted in figure 17(b), the rolling moments presented herein represent those for a full-span configuration where the right aileron is neutral ( $\delta_a = 0^\circ$ ) and the left aileron is at the given  $\delta_a$ .

With the flap deflected  $53^\circ$  and with blowing over the flap and aileron, a series of tests were conducted to determine the  $C_l$  produced for a left-aileron deflection of  $25^\circ$  to  $53^\circ$ . The rolling moment for this configuration is shown by the data of figure 17(a). Figure 17(b) compares the rolling moment obtained with blowing for a differential aileron deflection of  $10^\circ$  (right aileron deflected  $25^\circ$  and the left aileron deflected  $35^\circ$ ) with the rolling moment obtained without blowing for a left-aileron deflection of  $10^\circ$  with the flap neutral and deflected  $53^\circ$ . The superiority of the arrangement with blowing is quite marked.

The results presented in figures 16 and 17 have been cross-plotted and presented in figure 18 to show more clearly the aileron effectiveness obtained between angles of attack of  $0^\circ$  to  $20^\circ$ . The aileron effectiveness  $\frac{\Delta C_l}{\delta_a}$  represents the average effectiveness for the aileron

deflection range tested. In general, for aileron deflections of  $0^\circ$  to  $15^\circ$ , the aileron effectiveness, without blowing and with the flap neutral, is about 80 percent of the theoretical effectiveness estimated by the method of reference 13. Blowing over the aileron at  $C_Q = 0.020$  with the flap neutral just about doubled the aileron effectiveness. Up to an angle of attack of about  $15^\circ$ , the aileron effectiveness was about equal to that predicted by the theory of reference 13 for aileron deflections between  $25^\circ$  and  $53^\circ$  with  $\delta_f = 53^\circ$  and blowing over the aileron and flap at a  $C_Q = 0.022$ .

## SUMMARY OF RESULTS

An investigation has been conducted to determine the influence on the lift effectiveness of a trailing-edge flap of blowing a high-energy stream of air over the upper surface of the flap. Included in the investigation were measurements of the chordwise pressure distribution at one representative station on the flap and the effect on the aileron effectiveness of blowing air over the aileron. The more pertinent results may be summarized as follows:

1. With a slat and fences installed and a 47-percent-semispan flap deflected  $53^\circ$ , the maximum increments in lift coefficient obtained at  $0^\circ$  angle of attack and at maximum lift were 0.94 and 0.63, respectively, with blowing as compared to 0.39 and 0.12, respectively, without blowing. For a 70-percent-semispan flap deflected  $53^\circ$ , these increments were 1.14 and 0.68, respectively, with blowing as compared to 0.46 and 0.16, respectively, without blowing. Although no conclusive evidence was obtained in this exploratory investigation, it is believed that these increments in lift coefficient were not larger because the blowing air did not adhere well to the upper surface of the flap.

2. For blowing over a 47-percent-semispan flap deflected  $53^\circ$ , installation of a slat alleviated the early stalling tendencies of the outboard sections and produced an increment in the maximum lift coefficient of 0.63 as compared to 0.43 without a slat installed.

3. With blowing, at a flow coefficient of 0.022, over a 47-percent-semispan flap deflected  $53^\circ$  and a 23-percent-semispan aileron, the aileron effectiveness obtained through an aileron deflection range of  $25^\circ$  to  $53^\circ$  was about equal, up to an angle of attack of about  $15^\circ$ , to the aileron effectiveness predicted by theory. The aileron effectiveness obtained with blowing was a considerable improvement over the aileron effectiveness obtained without blowing for the same flap configuration.

4. Blowing air over the trailing-edge flap caused the flap chord force to become more negative, the flap normal force to increase, the flap chordwise center of pressure to move forward, and the flap hinge moment to increase.

Langley Aeronautical Laboratory,  
National Advisory Committee for Aeronautics,  
Langley Field, Va., February 17, 1954.



## REFERENCES

1. Schwler, W.: Lift Increase by Blowing Out Air, Tests on Airfoil of 12 Percent Thickness, Using Various Types of Flap. NACA TM 1148, 1947.
2. Rebuffet, P., and Poisson-Quinton, Ph.: Investigations of the Boundary-Layer Control on a Full Scale Swept Wing With Air Bled Off From the Turbojet. NACA TM 1331, 1952.
3. Barnett, U. Reed, Jr., and Lipson, Stanley: Effects of Several High-Lift and Stall-Control Devices on the Aerodynamic Characteristics of a Semispan  $49^\circ$  Sweptback Wing. NACA RM L52D17a, 1952.
4. Lipson, Stanley, and Barnett, U. Reed, Jr.: Comparison of Semispan and Full-Span Tests of a  $47.5^\circ$  Sweptback Wing With Symmetrical Circular-Arc Sections and Having Drooped-Nose Flaps, Trailing-Edge Flaps, and Ailerons. NACA RM L51H15, 1951.
5. Sivells, James C., and Salmi, Rachel M.: Jet-Boundary Corrections for Complete and Semispan Swept Wings in Closed Circular Wind Tunnels. NACA TN 2454, 1951.
6. DeYoung, John: Theoretical Antisymmetric Span Loading for Wings of Arbitrary Plan Form at Subsonic Speeds. NACA Rep. 1056, 1951. (Supersedes NACA TN 2140.)
7. Swanson, Robert S., and Toll, Thomas A.: Jet-Boundary Corrections for Reflection-Plane Models in Rectangular Wind Tunnels. NACA Rep. 770, 1943. (Supersedes NACA WR L-458.)
8. Page, Fredrick Handley: Towards Slower and Safer Flying, Improved Take-Off and Landing, and Cheaper Airports. Jour. R.A.S., vol. LIV, Dec. 1950, pp. 721-739.
9. DeYoung, John: Theoretical Symmetric Span Loading Due to Flap Deflection for Wings of Arbitrary Plan Form at Subsonic Speeds. NACA Rep. 1071, 1952. (Supersedes NACA TN 2278).
10. Salmi, Reino J.: Effects of Leading-Edge Devices and Trailing-Edge Flaps on Longitudinal Characteristics of Two  $47.7^\circ$  Sweptback Wings of Aspect Ratios 5.1 and 6.0 at a Reynolds Number of  $6.0 \times 10^6$ . NACA RM L50F20, 1950.
11. Whittle, Edward F., Jr., and Lipson, Stanley: Low-Speed, Large-Scale Investigation of Aerodynamic Characteristics of a Semispan  $49^\circ$  Sweptback Wing With a Fowler Flap in Combination With a Plain Flap, Slats, and Fences. NACA RM L53D09, 1953.

12. Harper, John J.: Investigation at Low Speed of 45° and 60° Sweptback, Tapered, Low-Drag Wings Equipped With Various Types of Full-Span, Trailing-Edge Flaps. NACA TN 2468, 1951.
13. Lowry, John G., and Schneider, Leslie E.: Estimation of Effectiveness of Flap-Type Controls on Sweptback Wings. NACA TN 1674, 1948.

TABLE I  
INDEX OF TEST CONDITIONS AND CONFIGURATIONS

R	$\delta_f$ , deg	$\delta_a$ , deg	Slat span, b/2	Fence location, b/2	$C_Q$	Data presented	Figure
$6.1 \times 10^6$	0 30 45 53 60	0	Off	Off	0	$C_L$ against $\alpha$ $C_D$ } against $C_L$ $C_m$ } $y_{cp}$ }	4
6.1	30 45 53 60	0	Off	Off	.02	$C_L$ against $\alpha$ $C_D$ } against $C_L$ $C_m$ } $y_{cp}$ }	5
6.1 6.1 4.4 2.9	45	0	Off	Off	0 .020 .030 .043	$C_L$ against $\alpha$ $C_D$ } against $C_L$ $C_m$ } $y_{cp}$ }	6
6.1 4.4 6.1 4.4	53	0	Off	Off	0 0 .020 .030	$C_L$ against $\alpha$ $C_D$ } against $C_L$ $C_m$ } $y_{cp}$ }	7
4.4	53	0	Off .5	Off .6, .8	0	$C_L$ against $\alpha$ $C_D$ } against $C_L$ $C_m$ } $y_{cp}$ }	8
4.4	53	0	Off .5	Off .6, .8	.03	$C_L$ against $\alpha$ $C_D$ } against $C_L$ $C_m$ } $y_{cp}$ }	9
4.4	30 53	0	.5	.6	.03	$C_L$ against $\alpha$ $C_D$ } against $C_L$ $C_m$ } $y_{cp}$ }	10
4.4 2.9 4.4 4.4 2.9	53	0	.5	.6, .8	0 0 .022 .029 .042	$C_L$ against $\alpha$ $C_D$ } against $C_L$ $C_m$ } $y_{cp}$ }	11



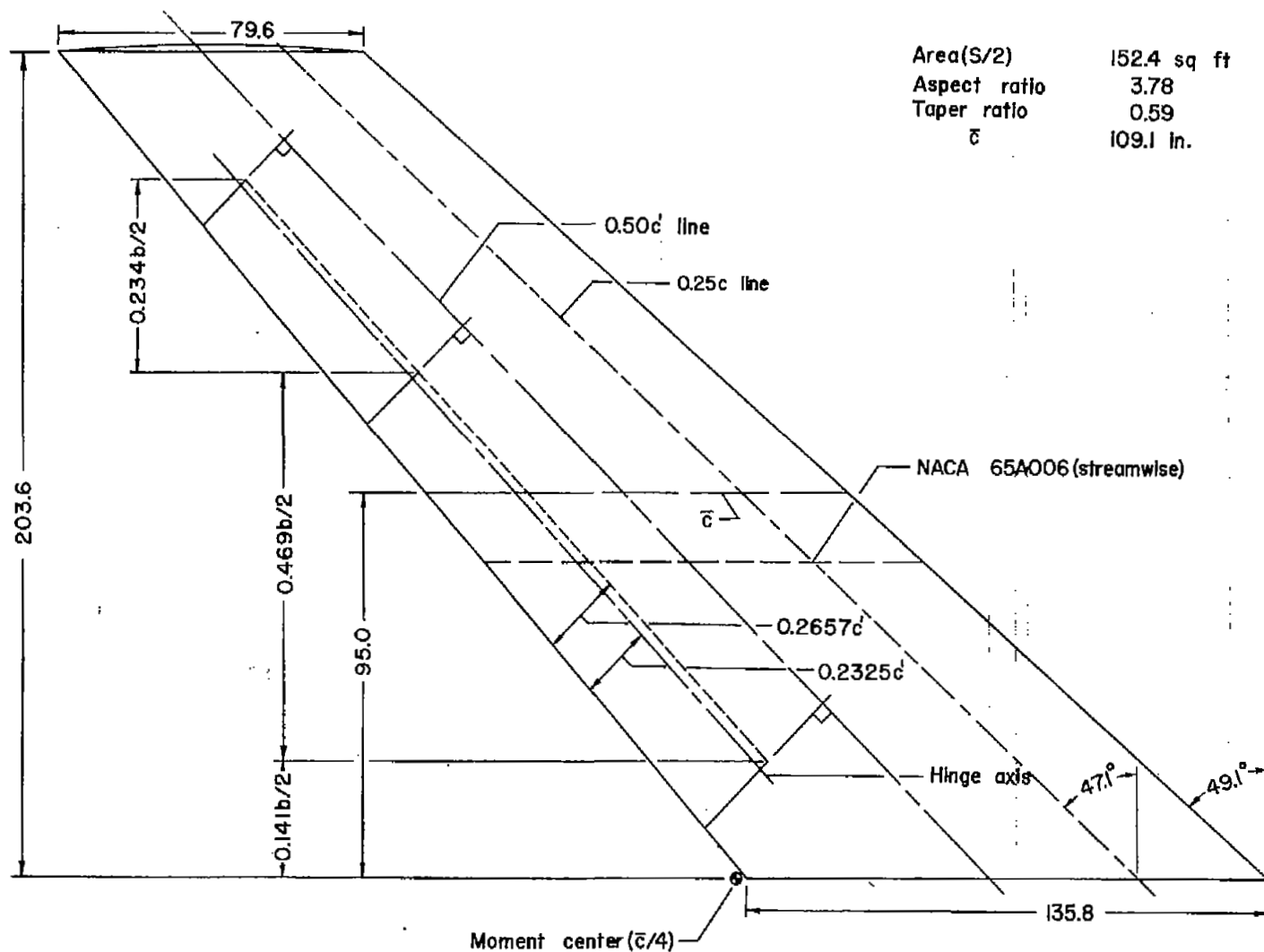


Figure 1.- Plan form of the semispan 49.1° sweptback wing. All dimensions are given in inches unless otherwise noted.

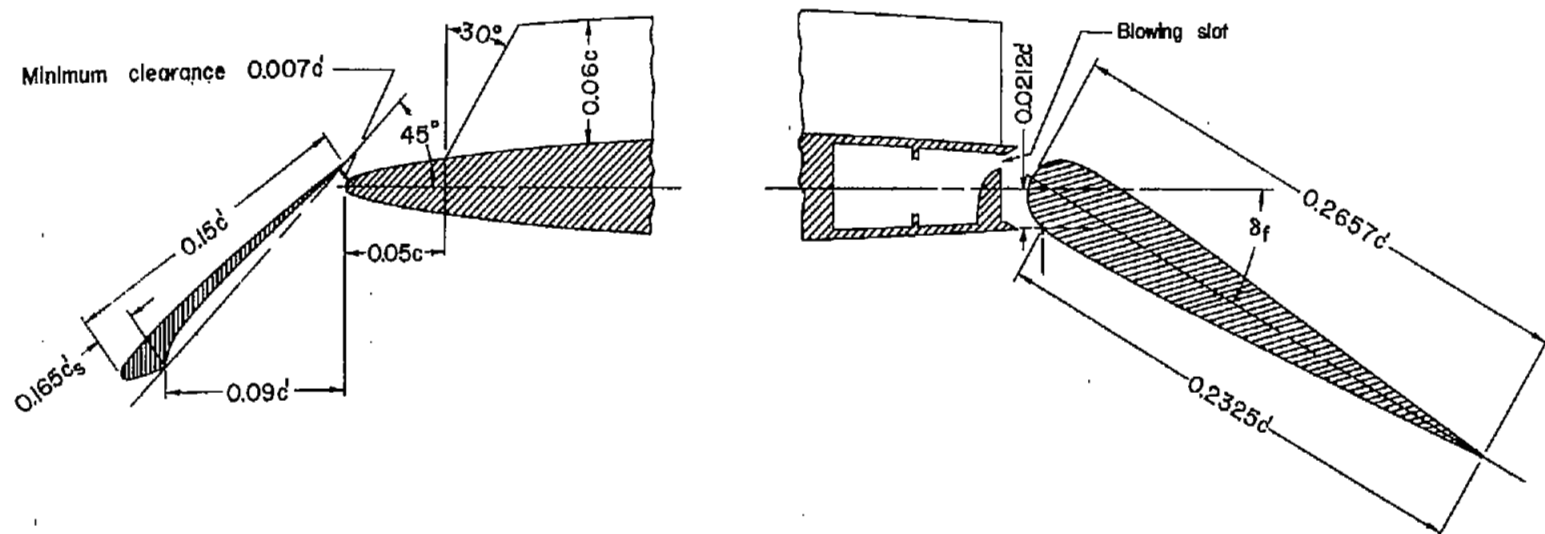
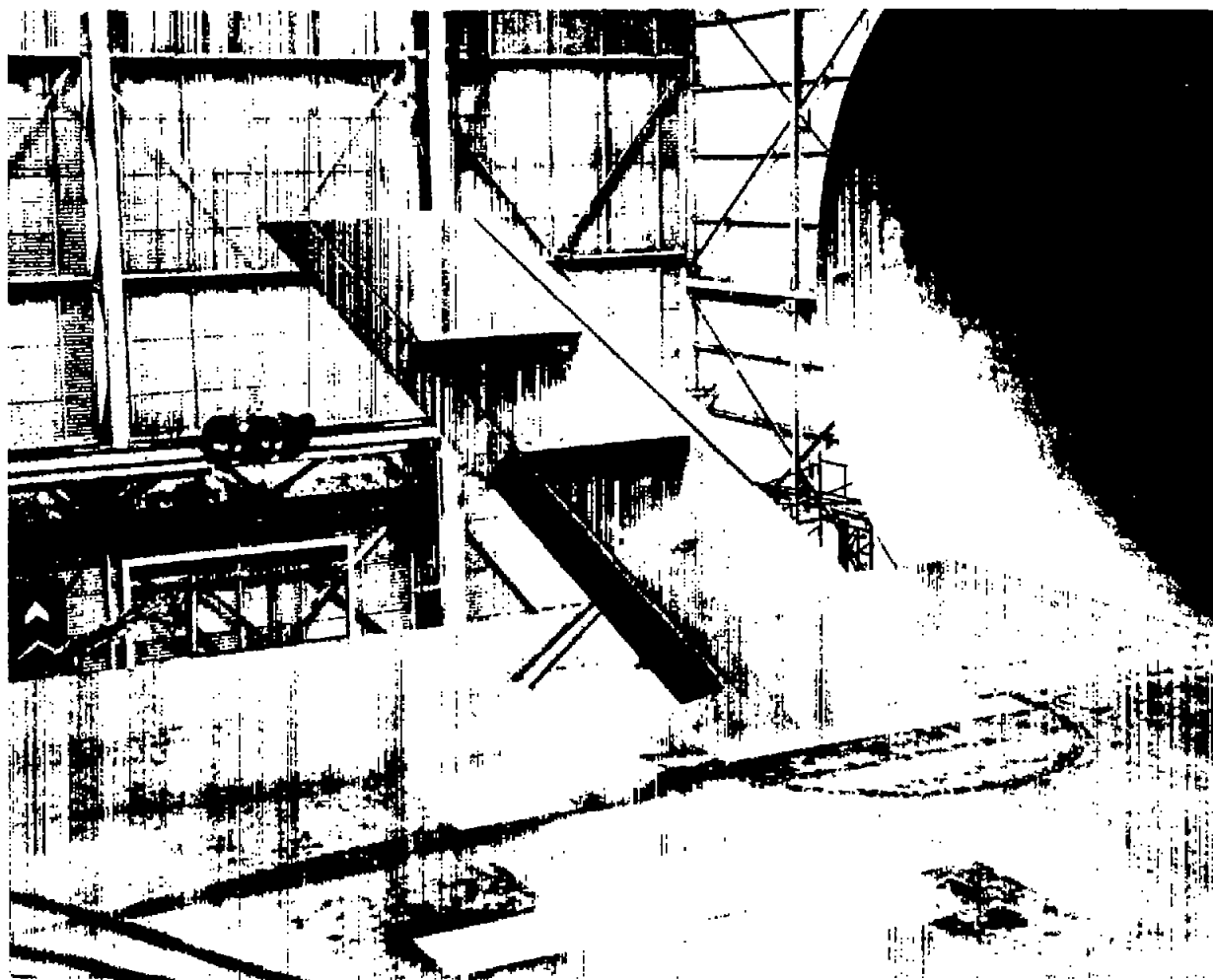


Figure 2.- Details of the slat, fences, and flap.



L-76748

Figure 3.-- The semispan  $49.1^\circ$  sweptback wing, with a  $0.47b/2$  plain flap deflected, a  $0.5b/2$  slat installed, and fences located at  $0.6b/2$  and  $0.8b/2$ , mounted on the reflection plane in the Langley full-scale tunnel.

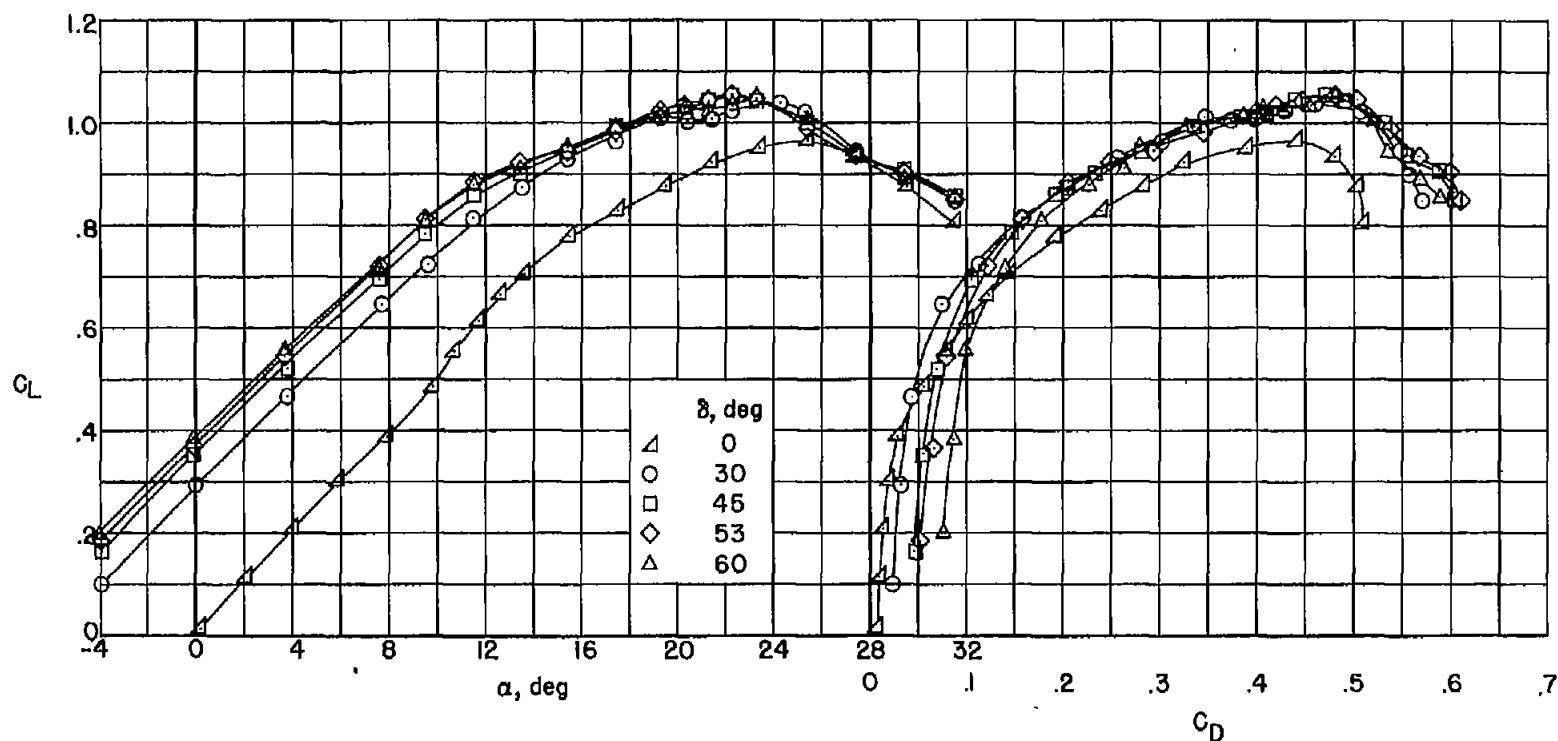


Figure 4.- Effect on aerodynamic characteristics of the semispan 49.1° sweptback wing of flap deflection. Basic wing;  $\delta_B = 0$ ;  $C_Q = 0$ ;  $R = 6.1 \times 10^6$ .



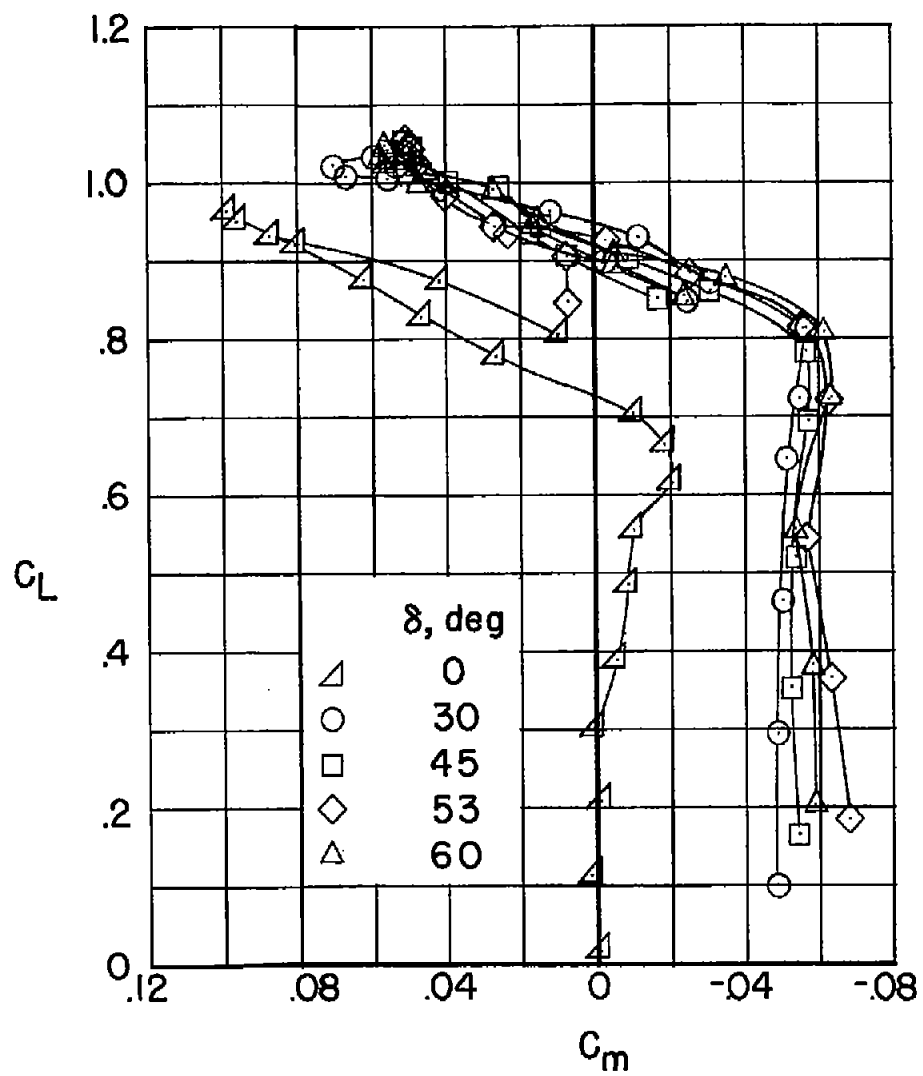
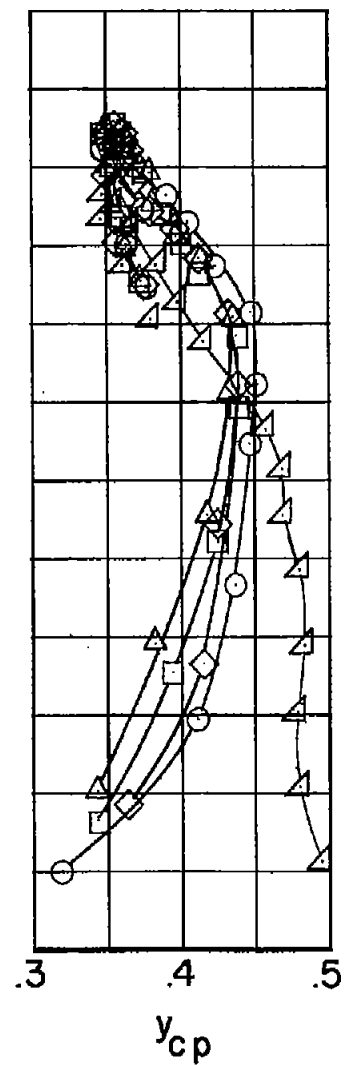


Figure 4.- Concluded.



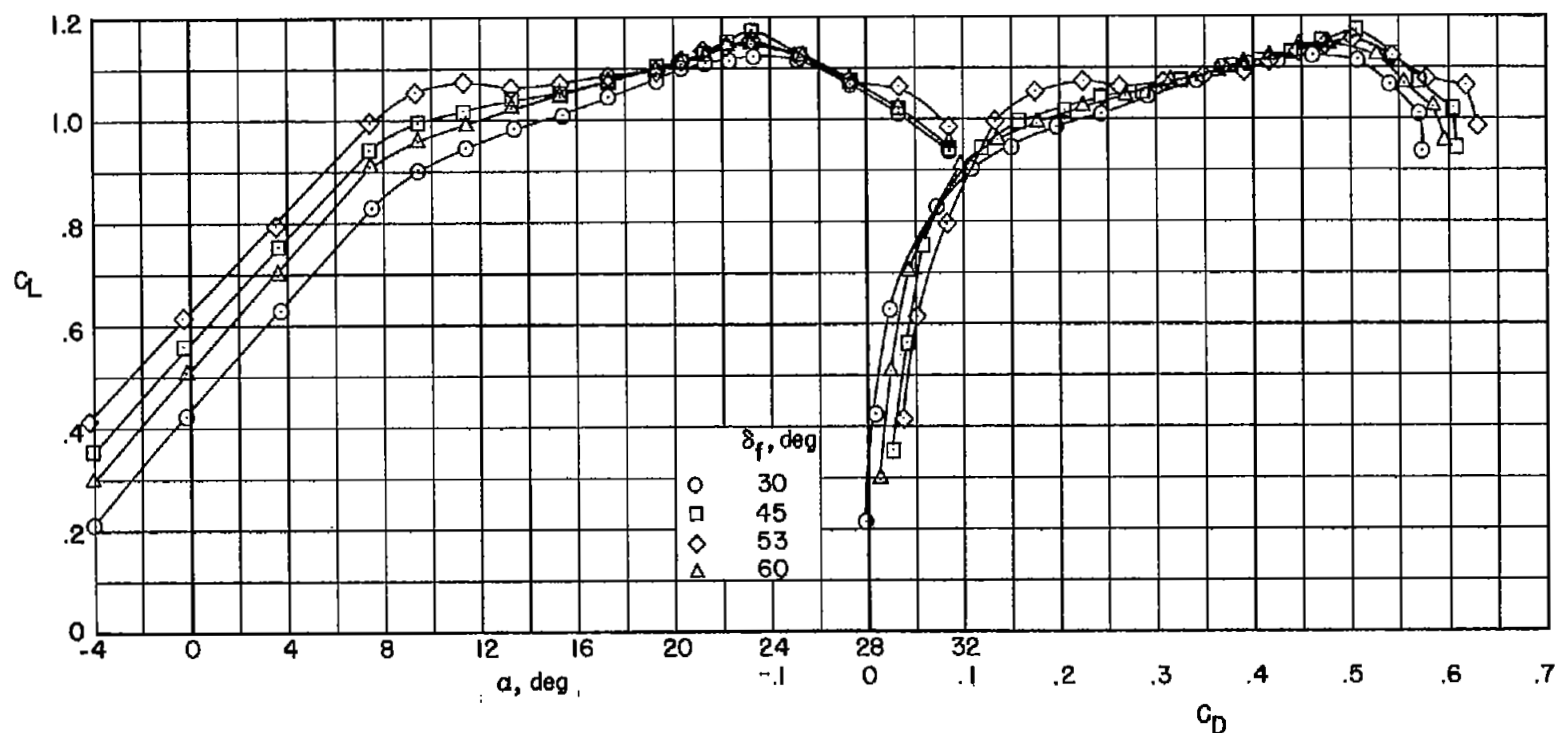


Figure 5.- Effect on aerodynamic characteristics of the semispan 49.1° sweptback wing of flap deflection. Basic wing;  $\delta_a = 0$ ;  $C_Q \approx 0.02$ ;  $R = 6.1 \times 10^6$ .

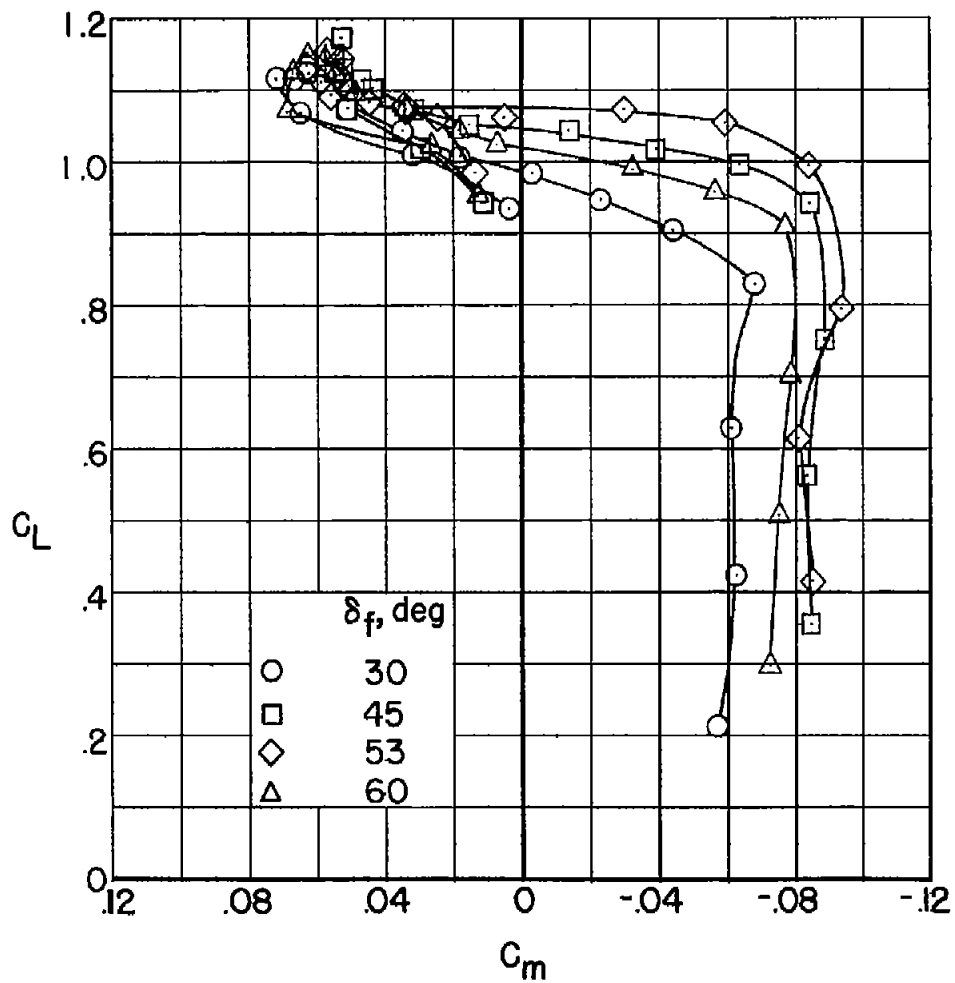
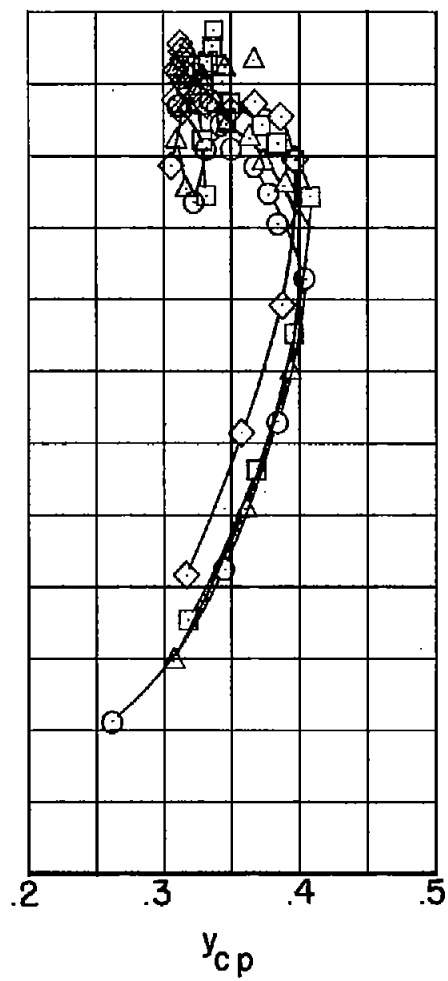


Figure 5.- Concluded.



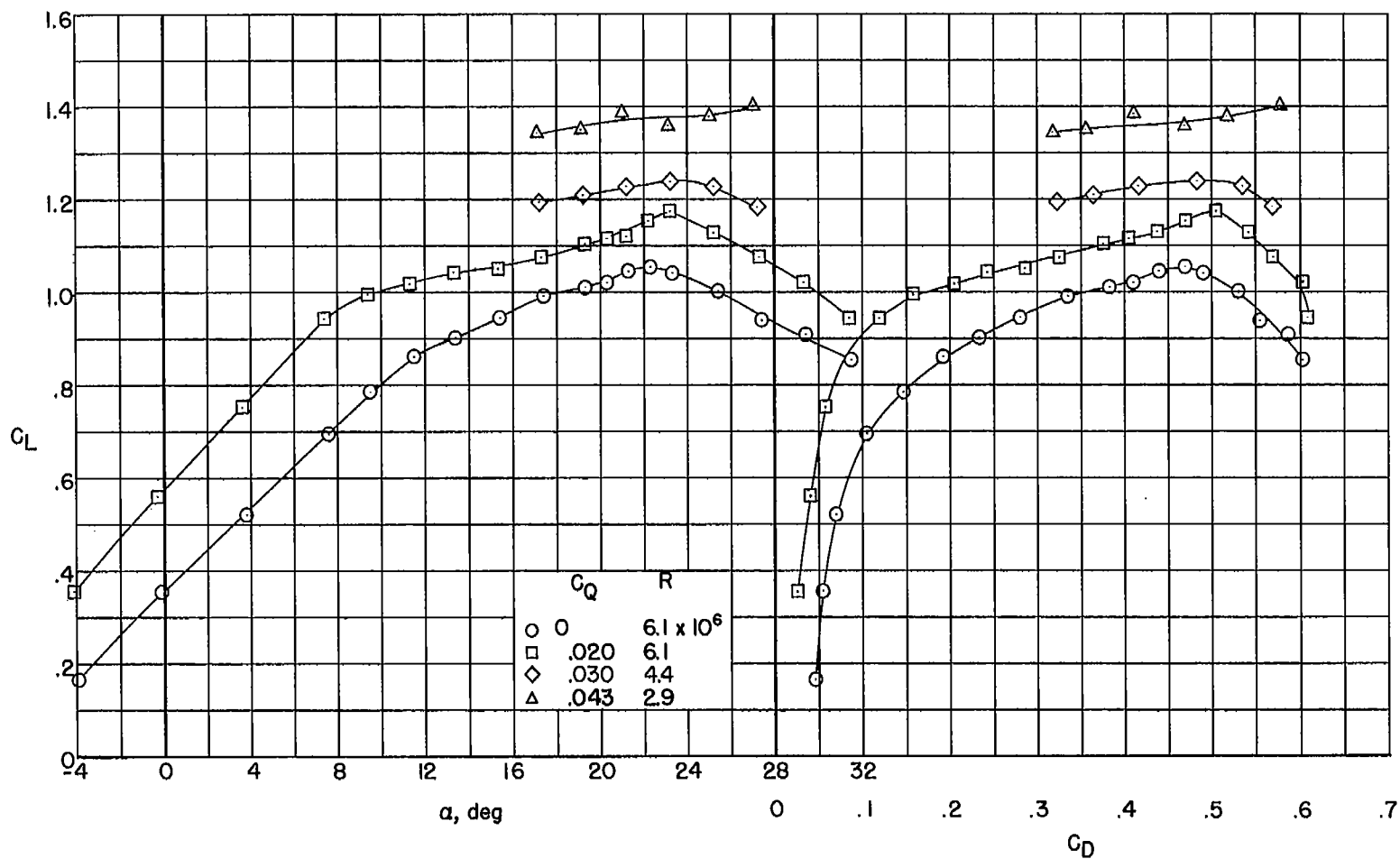


Figure 6.- Effect on aerodynamic characteristics of the semispan  $49.1^\circ$  sweptback wing of  $C_Q$ . Basic wing;  $\delta_f = 45^\circ$ ;  $\delta_a = 0^\circ$ .

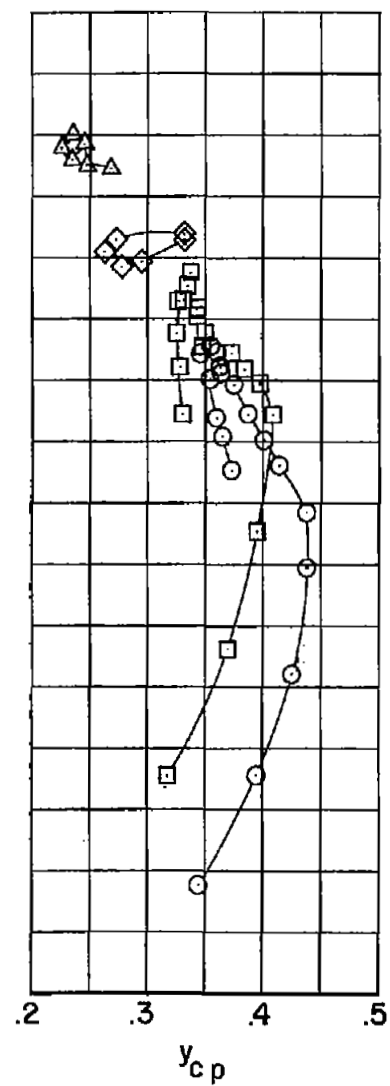
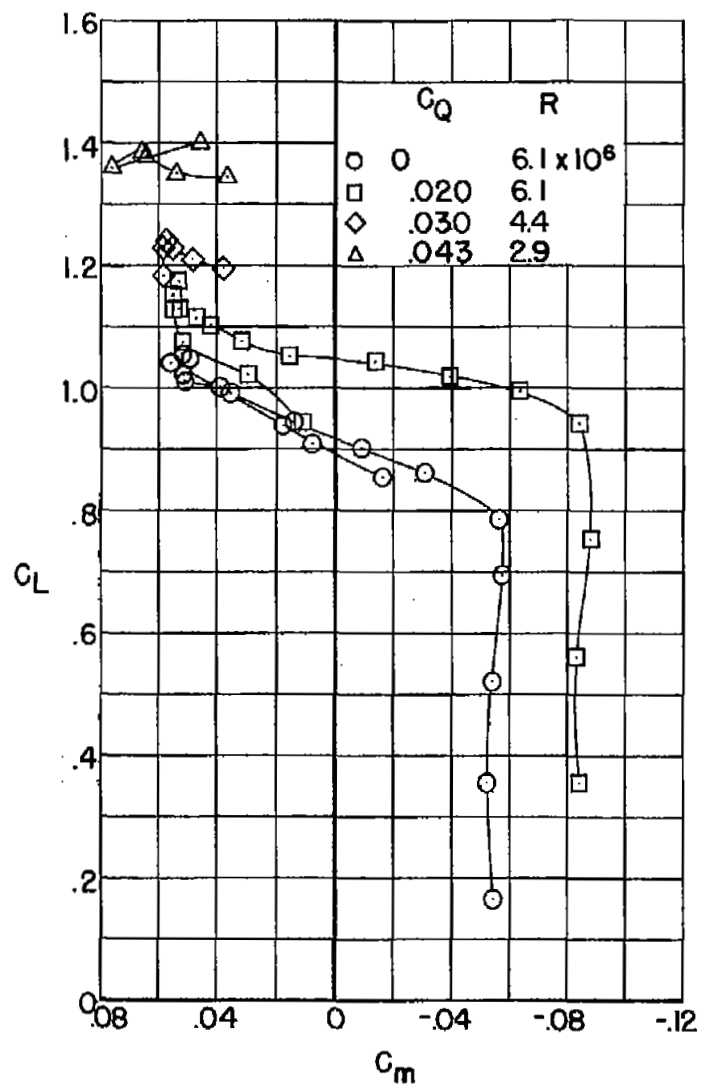


Figure 6.- Concluded.

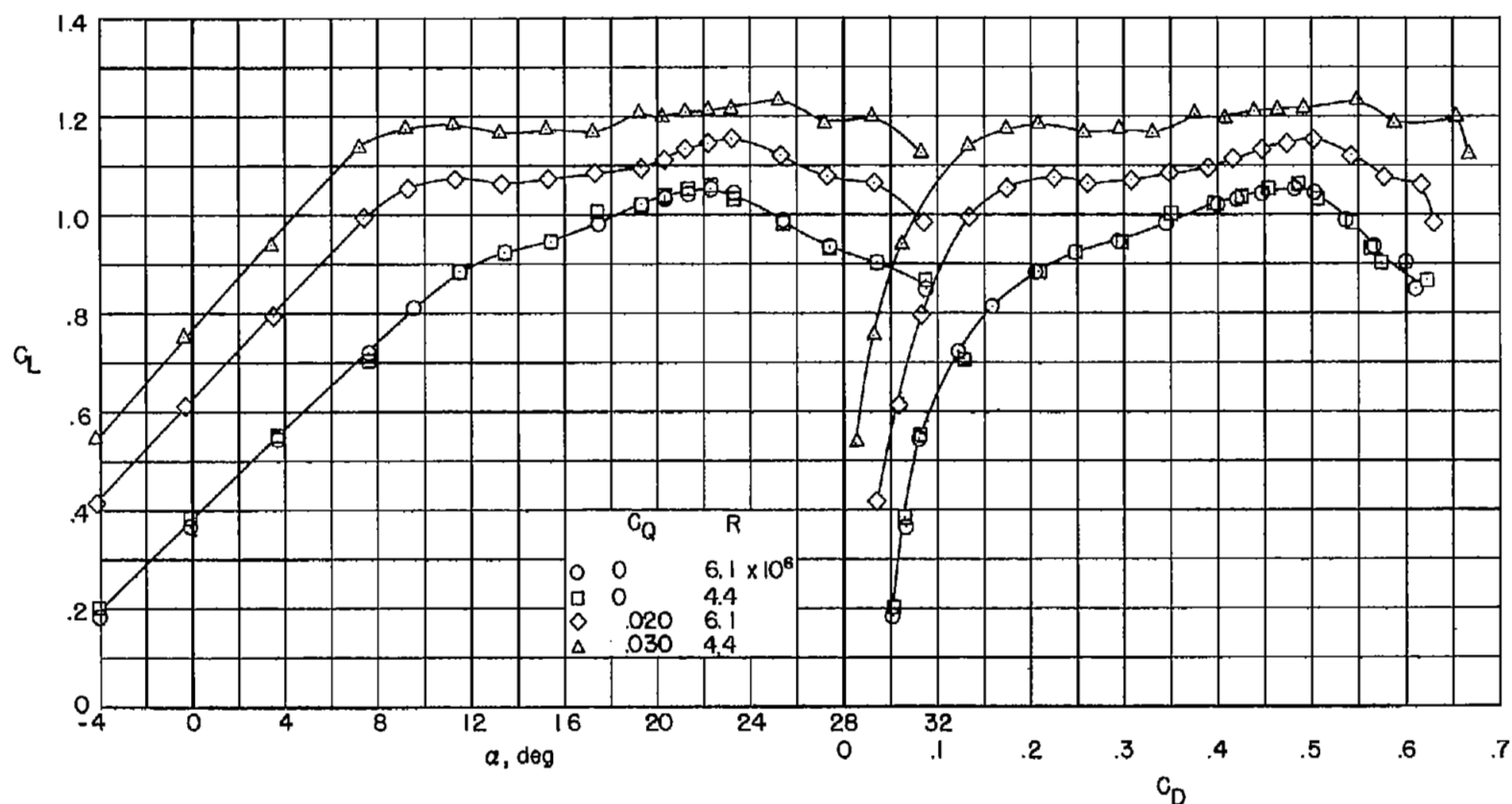


Figure 7.- Effect on aerodynamic characteristics of the semispan 49.1° sweptback wing of  $C_Q$ . Basic wing;  $\delta_f = 53^\circ$ ;  $\delta_a = 0^\circ$ .

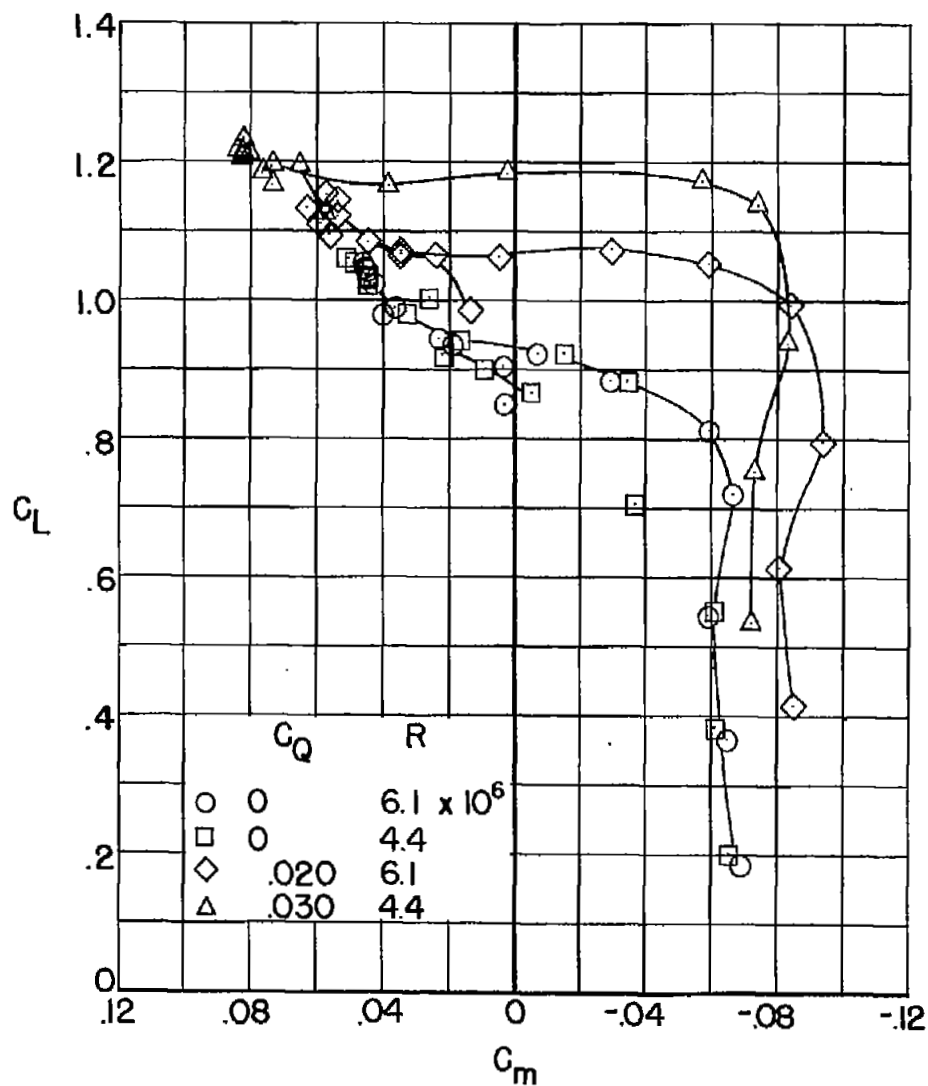
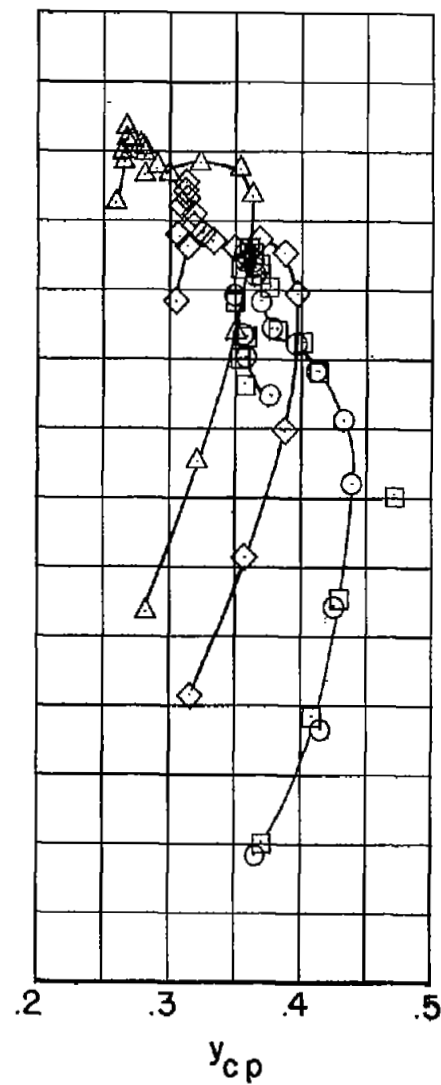


Figure 7.- Concluded.



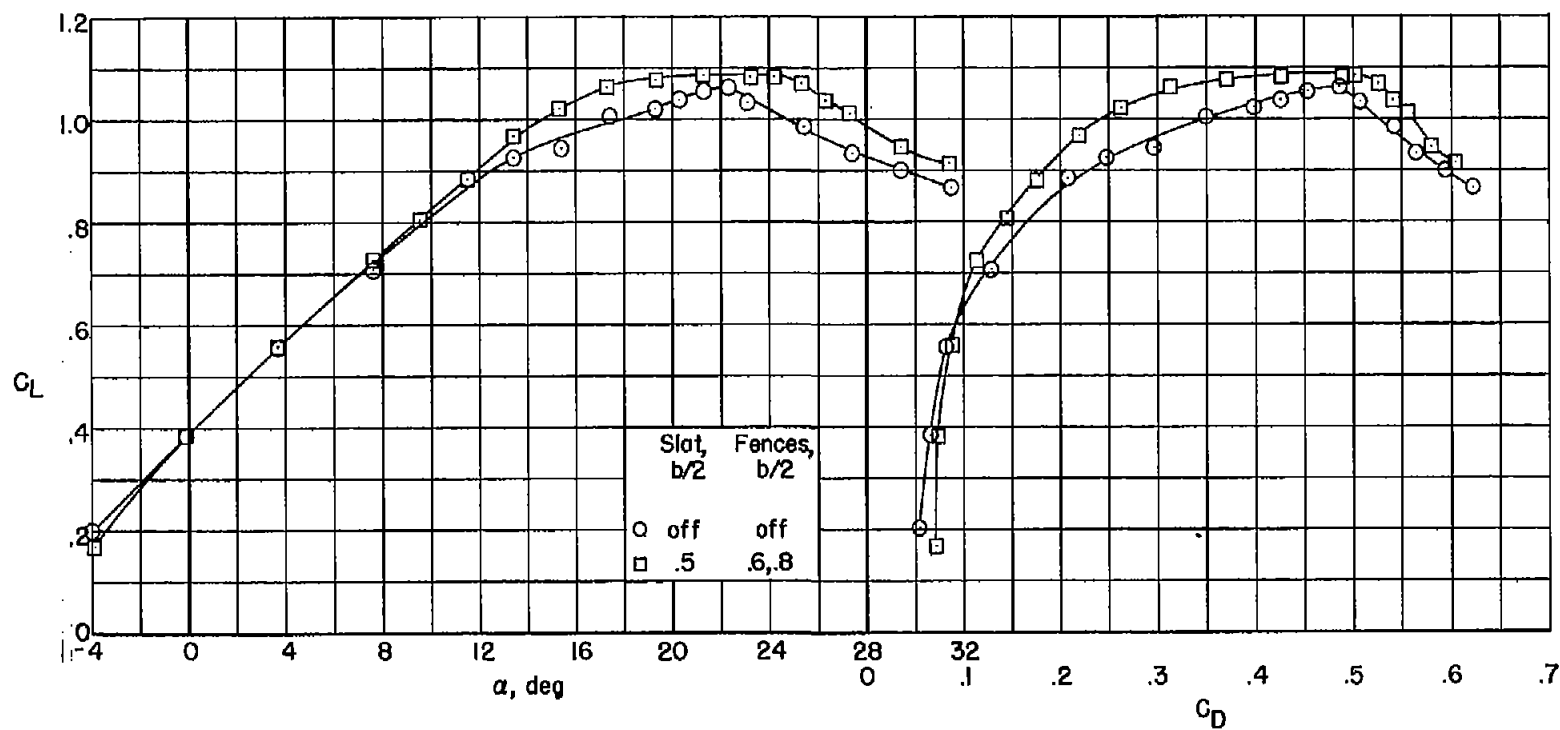


Figure 8.- Effect on aerodynamic characteristics of the semispan  
 49.1° sweptback wing of delaying tip stall.  $\delta_f = 53^\circ$ ;  $\delta_a = 0^\circ$ ;  
 $C_Q = 0$ ;  $R = 4.4 \times 10^6$ .



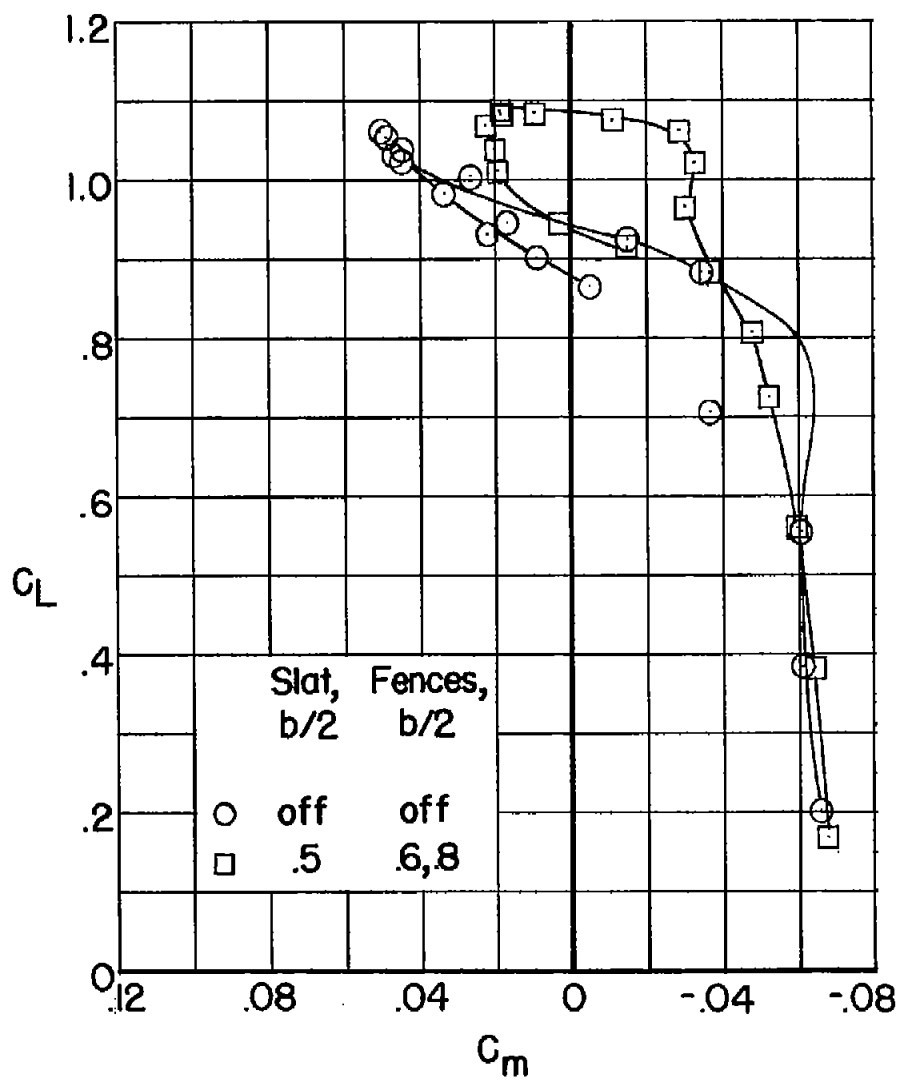
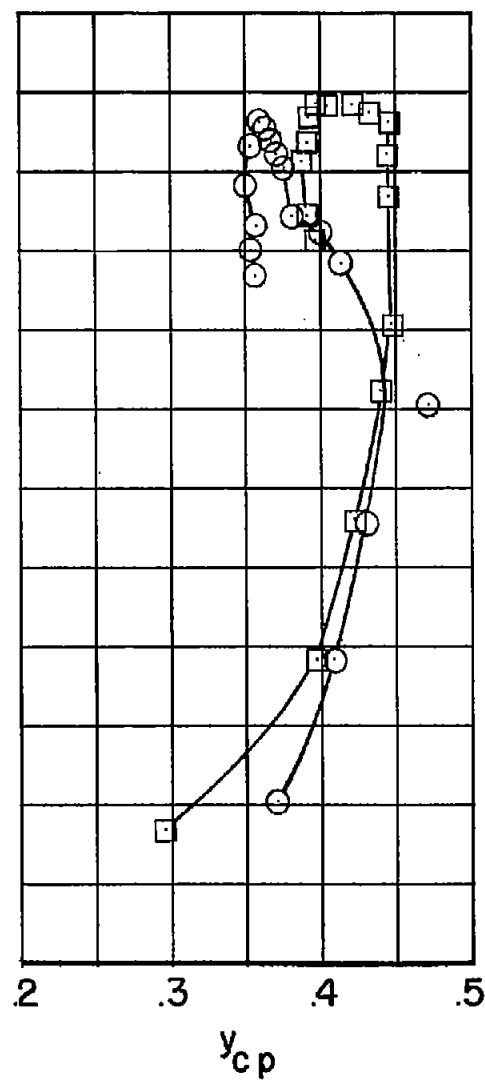


Figure 8.- Concluded.



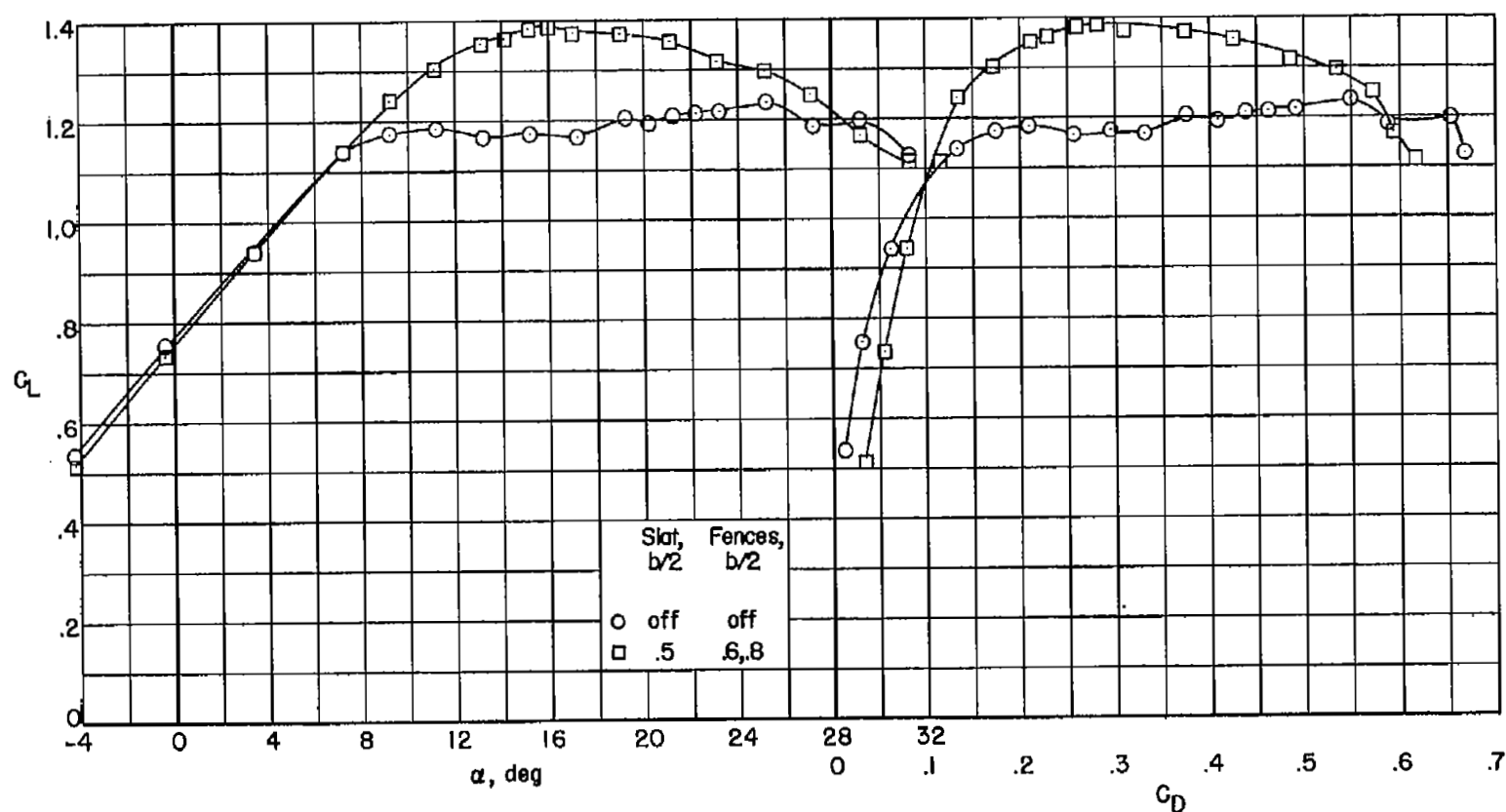


Figure 9.- Effect on aerodynamic characteristics of the semispan 49.1° sweptback wing of delaying tip stall.  $\delta_f = 53^\circ$ ;  $\delta_a = 0^\circ$ ;  $C_Q \approx 0.03$ ;  $R = 4.4 \times 10^6$ .

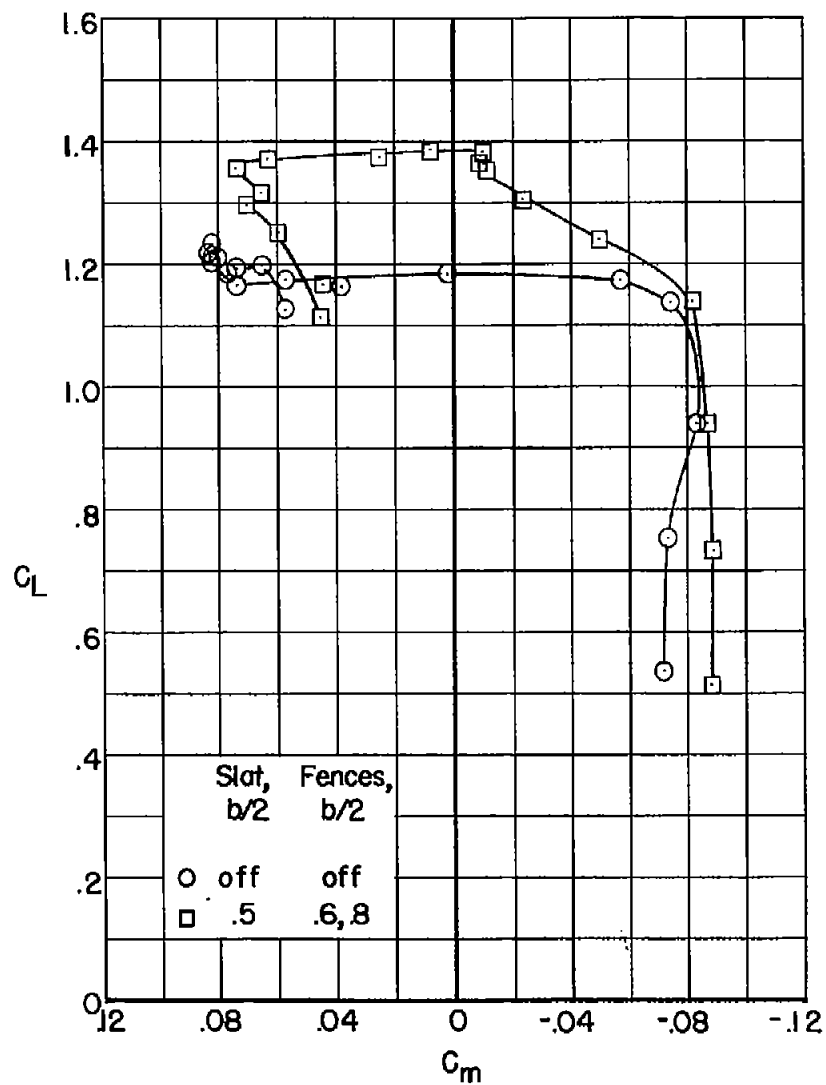
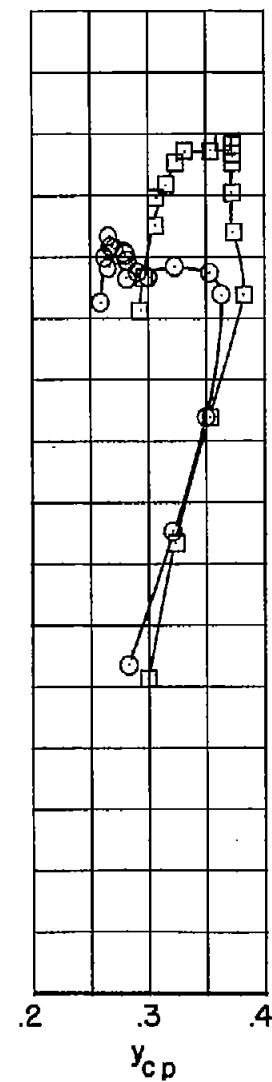


Figure 9.- Concluded.



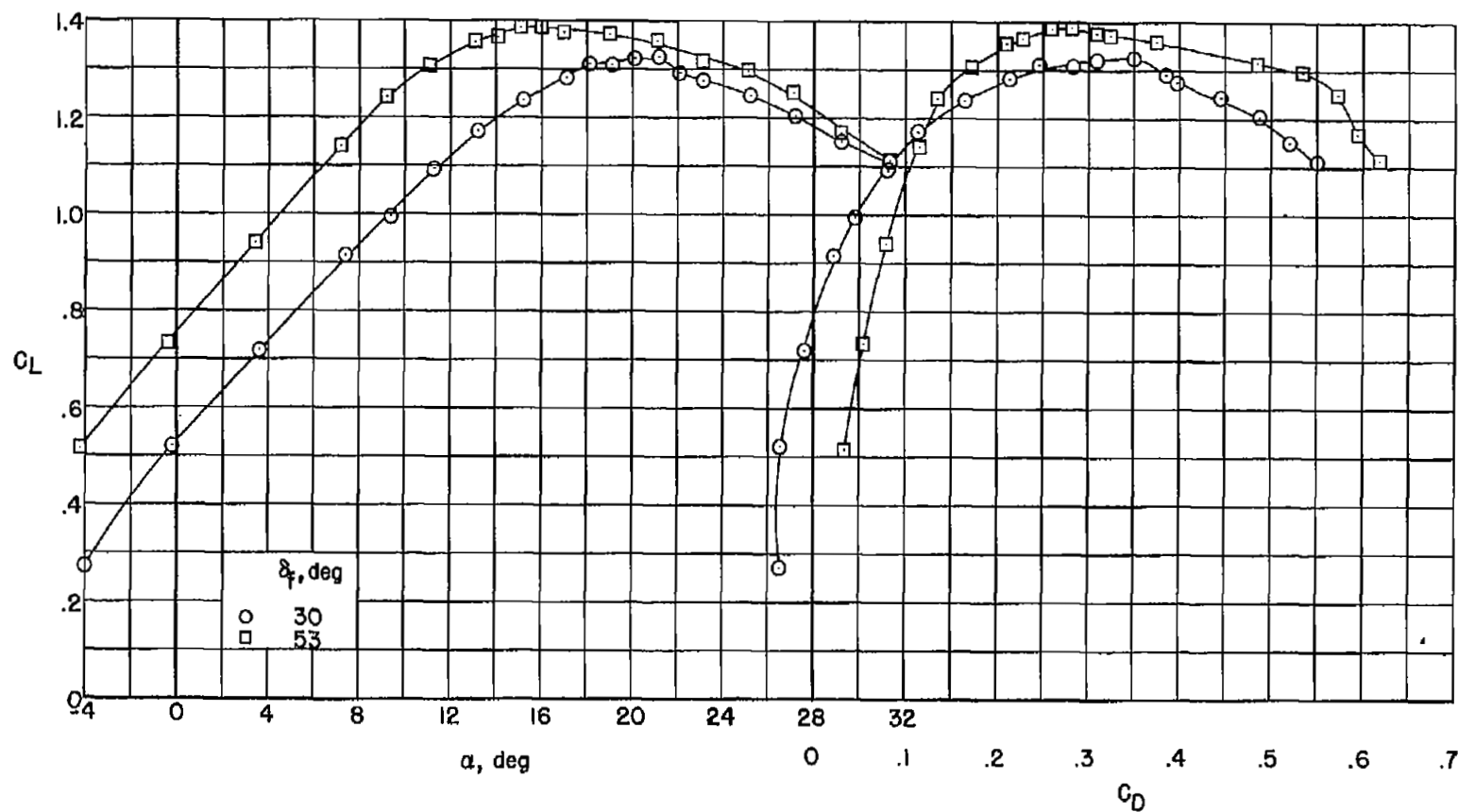


Figure 10.- Effect on aerodynamic characteristics of the semispan 49.1° sweptback wing of flap deflection.  $\delta_a = 0^\circ$ ;  $0.5b/2$  slat;  $0.6b/2$  fences;  $C_Q \approx 0.03$ ;  $R = 4.4 \times 10^6$ .

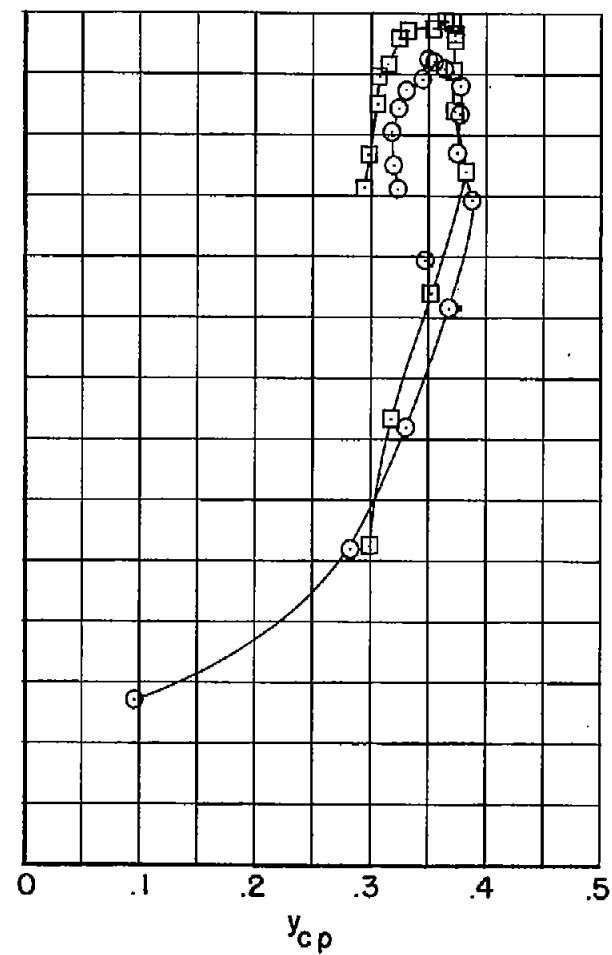
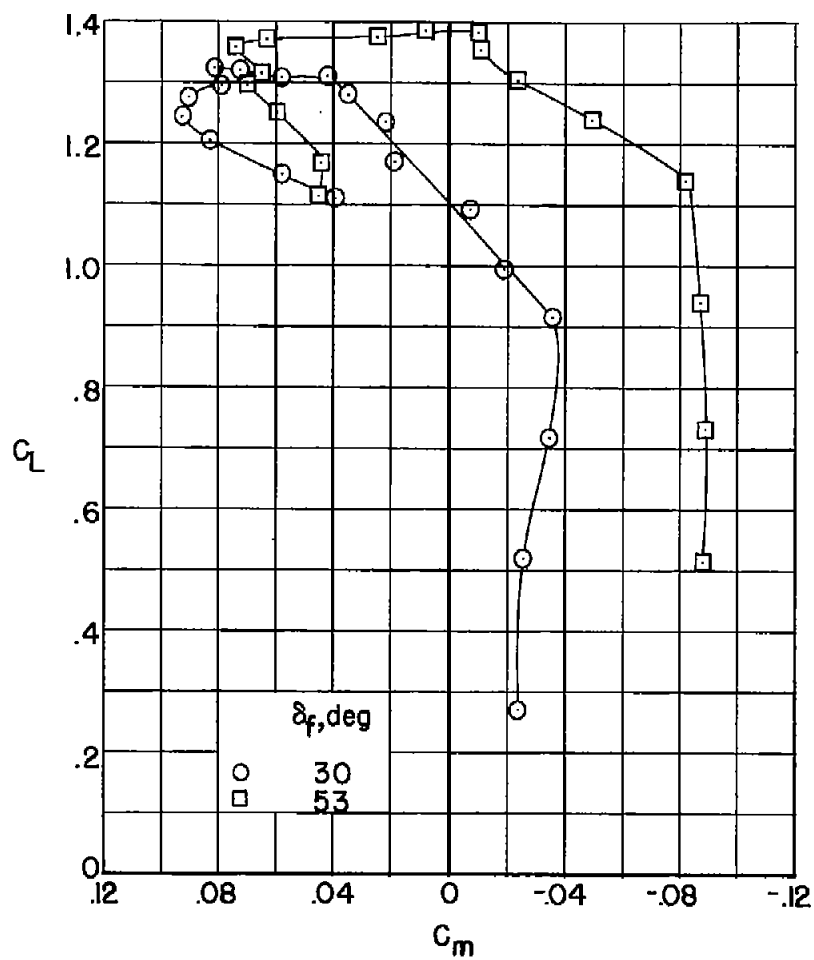


Figure 10.- Concluded.

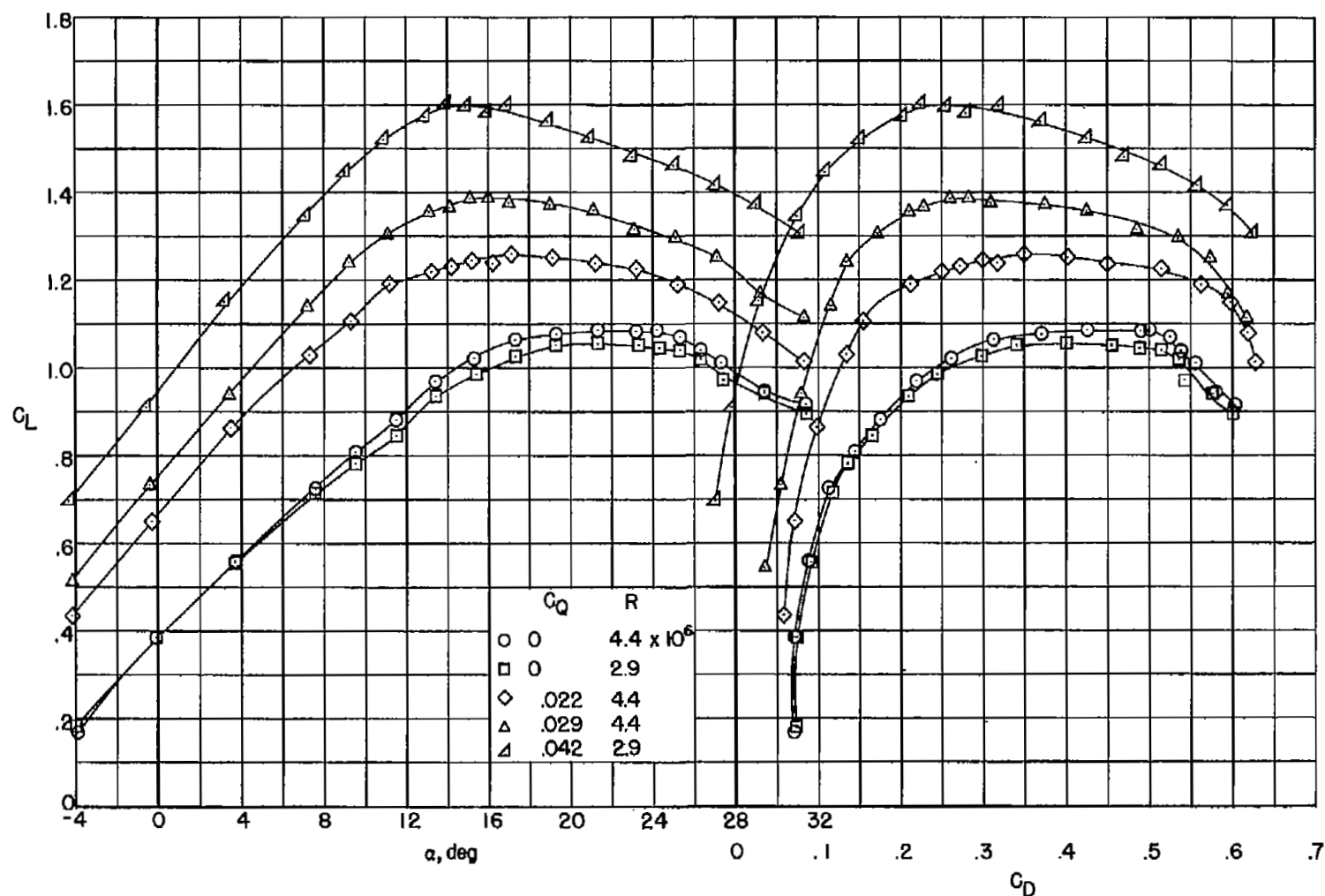


Figure 11.- Effect on aerodynamic characteristics of the semispan  
 49.1° sweptback wing of  $C_Q$ . 0.5b/2 slat; 0.6b/2 and 0.8b/2 fences;  
 $\delta_F = 53^\circ$ ;  $\delta_A = 0^\circ$ .

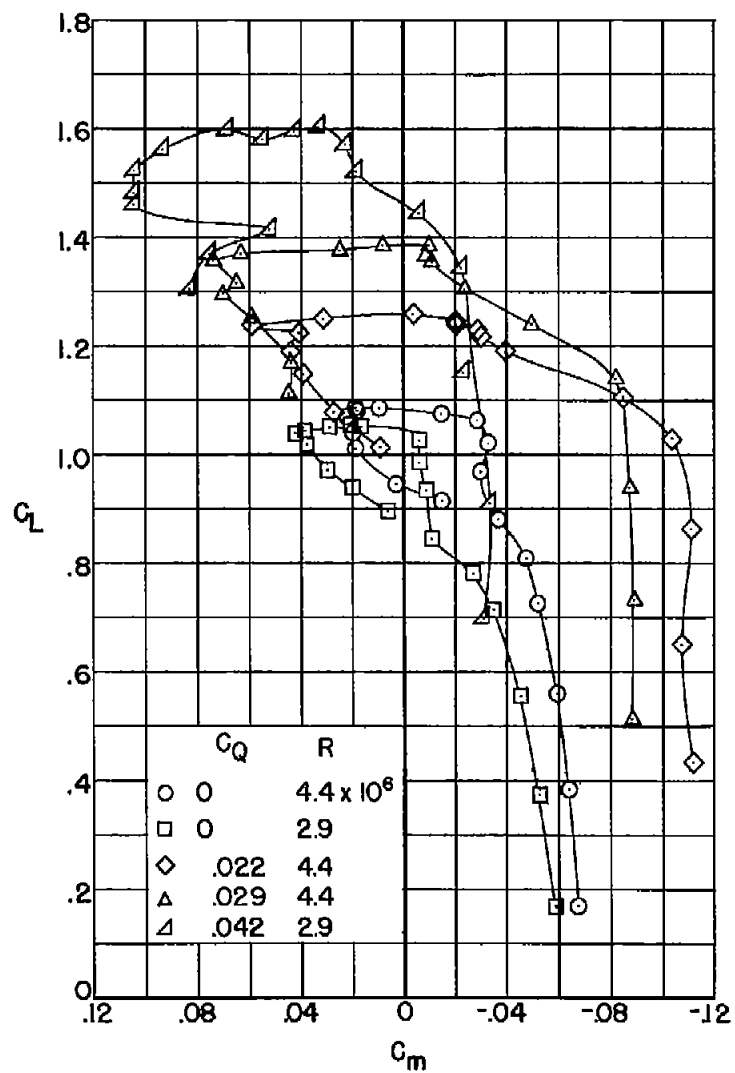
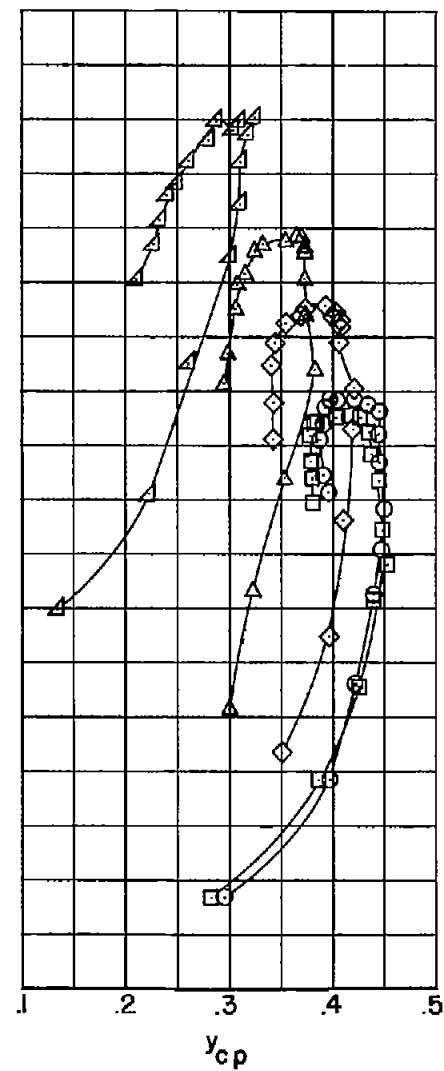


Figure 11.- Concluded.



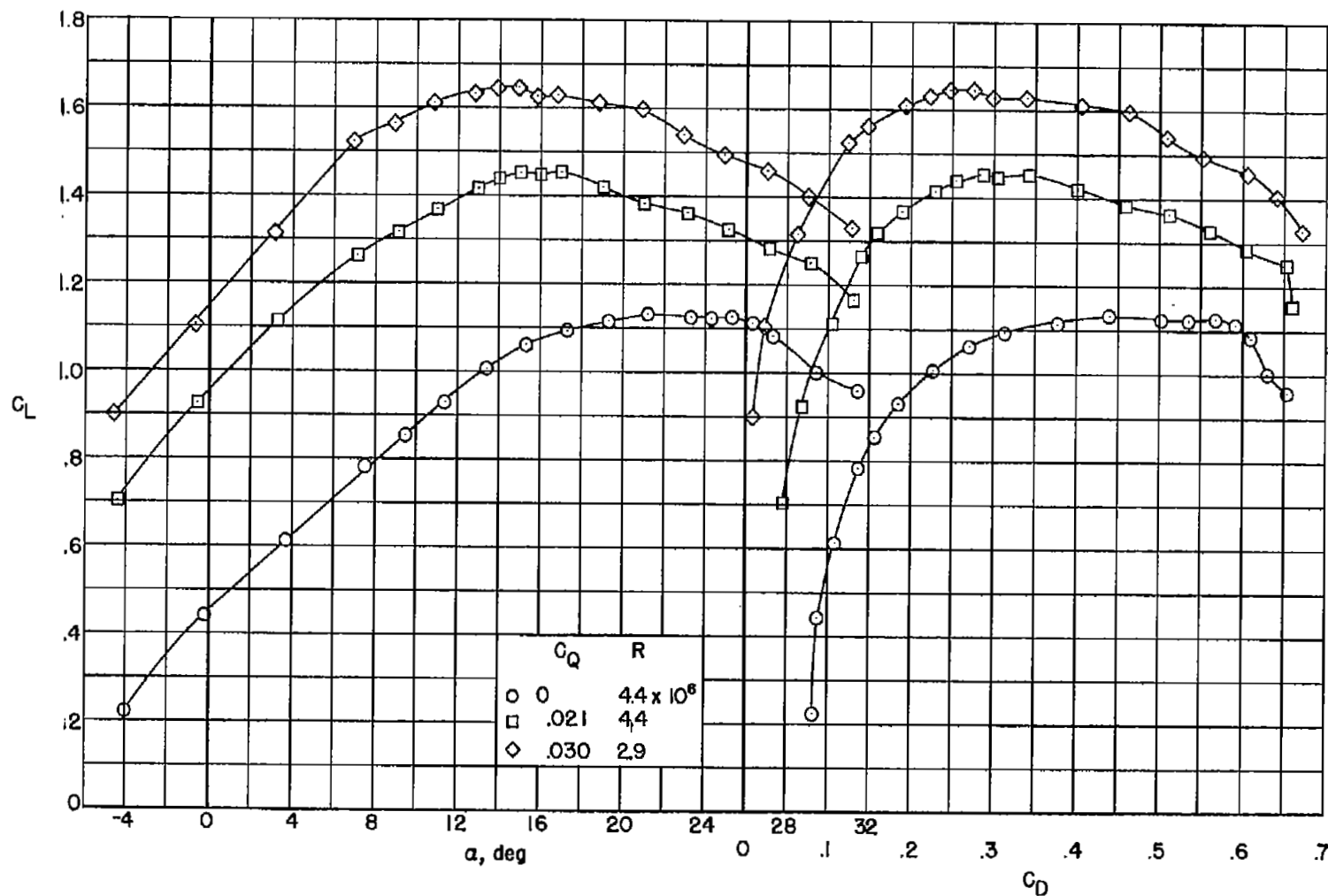


Figure 12.- Effect on aerodynamic characteristics of the semispan  $49.1^\circ$  sweptback wing of  $C_Q$ .  $\delta_f = 53^\circ$ ;  $\delta_a = 53^\circ$ ;  $0.5b/2$  slat;  $0.6b/2$  and  $0.8b/2$  fences.



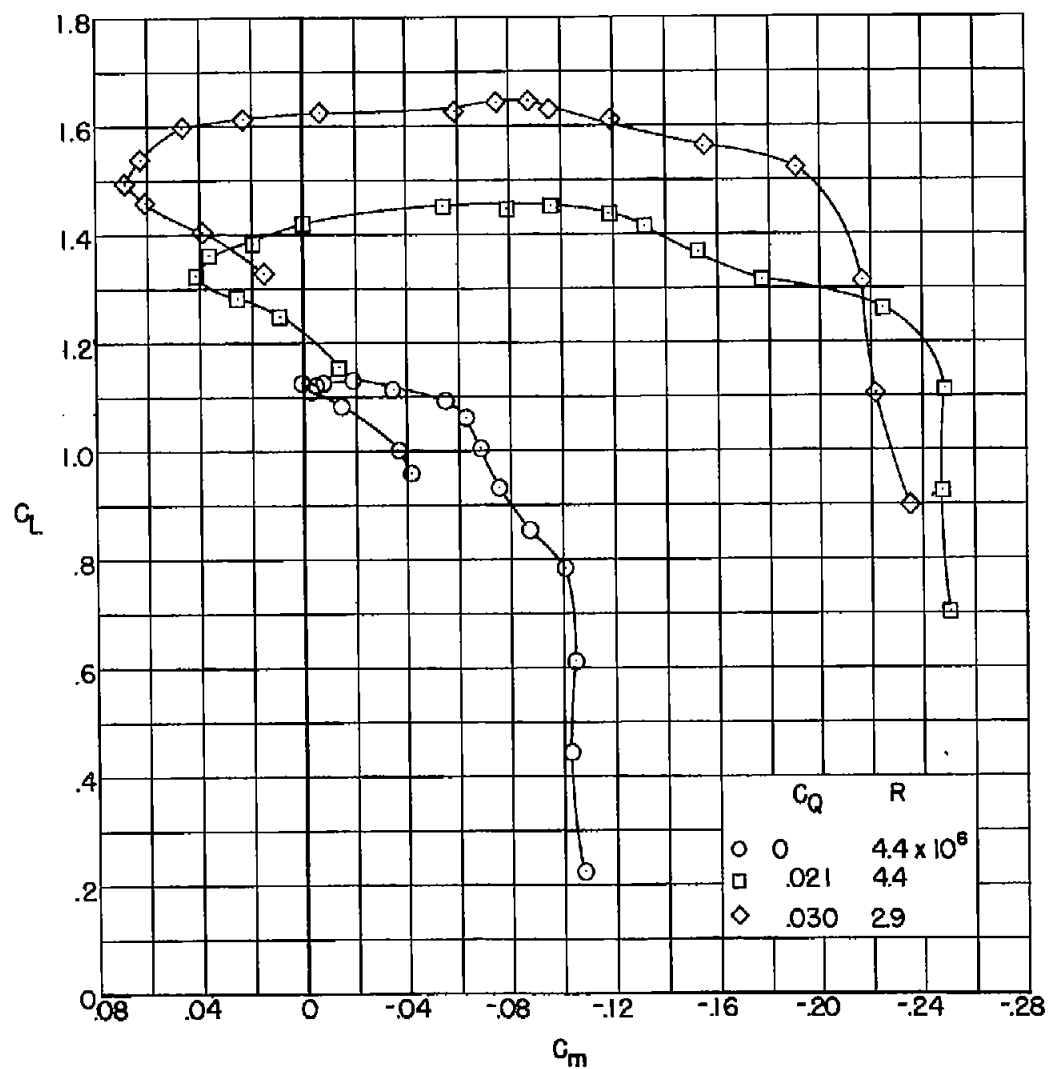
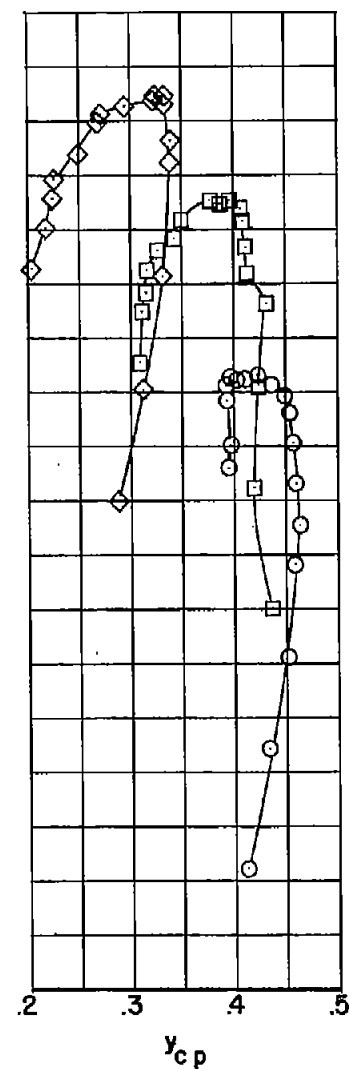
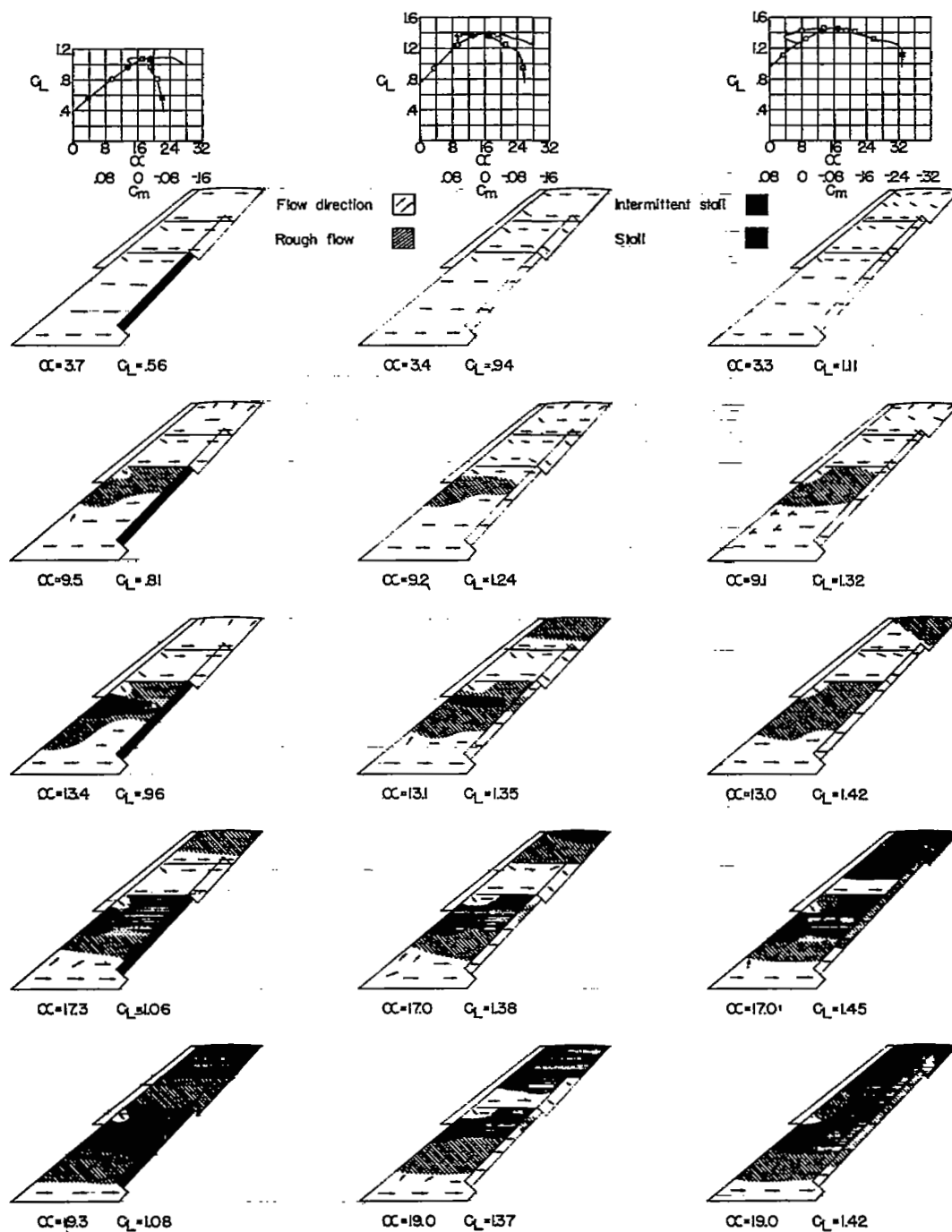


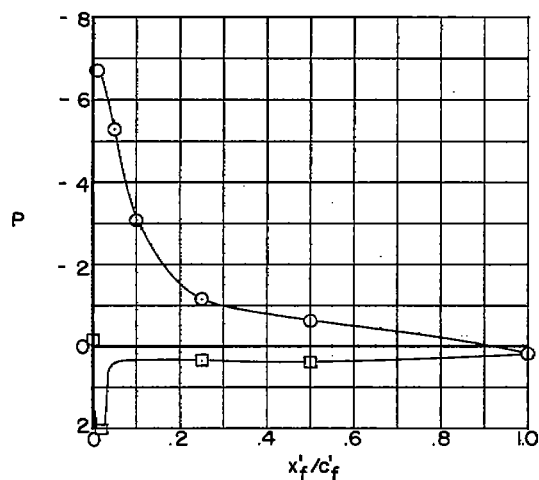
Figure 12.- Concluded.



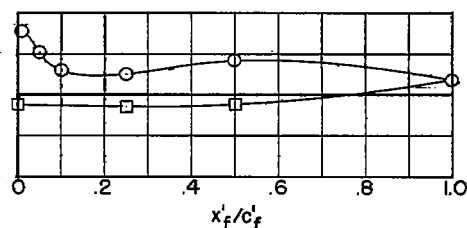


(a)  $C_Q = 0$ ;  $\delta_F = 53^\circ$ ;  $\delta_A = 0^\circ$ . (b)  $C_Q \approx 0.03$ ;  $\delta_F = 53^\circ$ ;  $\delta_A = 0^\circ$ . (c)  $C_Q \approx 0.02$ ;  $\delta_F = 53^\circ$ ;  $\delta_A = 53^\circ$ .

Figure 13.- Flow studies with and without blowing over the trailing-edge flaps.  $0.5b/2$  slat;  $0.6b/2$  and  $0.8b/2$  fences;  $R = 4.4 \times 10^6$ .

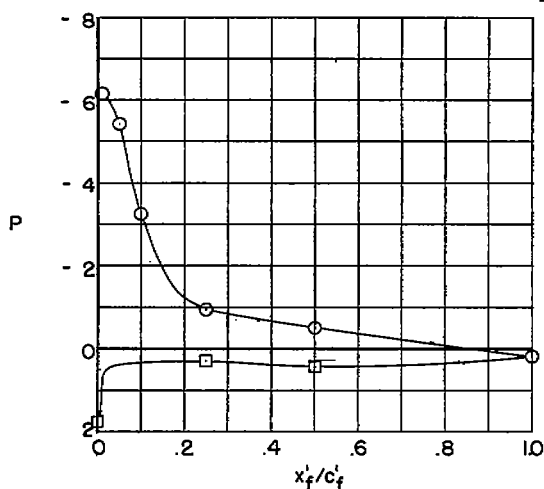


(a)  $\delta_f = 53^\circ$ ; slat off; fences off;  
 $C_Q = 0.03$ ;  $C_L = 1.16$ .

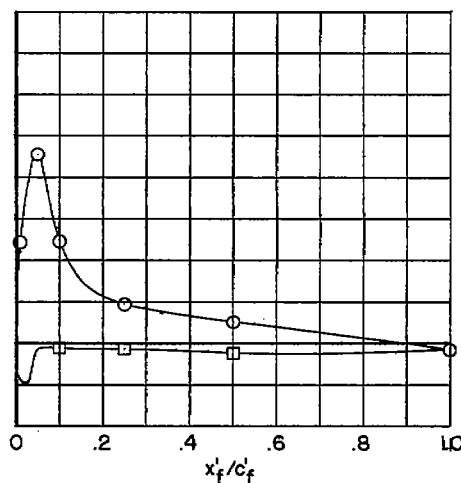


(b)  $\delta_f = 53^\circ$ ; slat off; fences off;  
 $C_Q = 0$ ;  $C_L = 0.94$ .

○ Upper surface  
□ Lower surface



(c)  $\delta_f = 53^\circ$ ;  $0.5b/2$  slat;  $0.6b/2$   
and  $0.8b/2$  fences;  $C_Q = 0.03$ ;  
 $C_L = 1.34$ .



(d)  $\delta_f = 30^\circ$ ;  $0.5b/2$  slat;  $0.6b/2$   
and  $0.8b/2$  fences;  $C_Q = 0.03$ ;  
 $C_L = 1.23$ .

Figure 14.- Typical pressure distributions on the trailing-edge flap.  
 $\alpha \approx 15.2^\circ$ ;  $\delta_a = 0^\circ$ ;  $R = 4.4 \times 10^6$ .

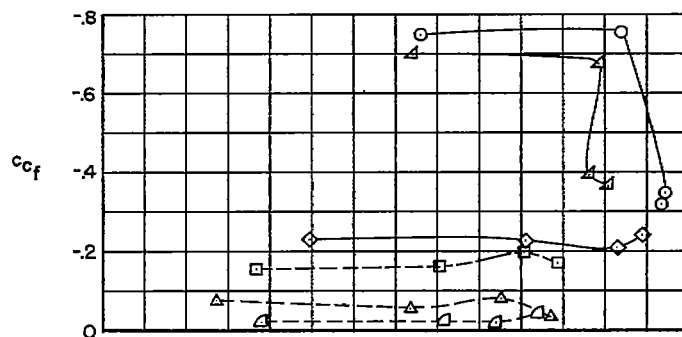
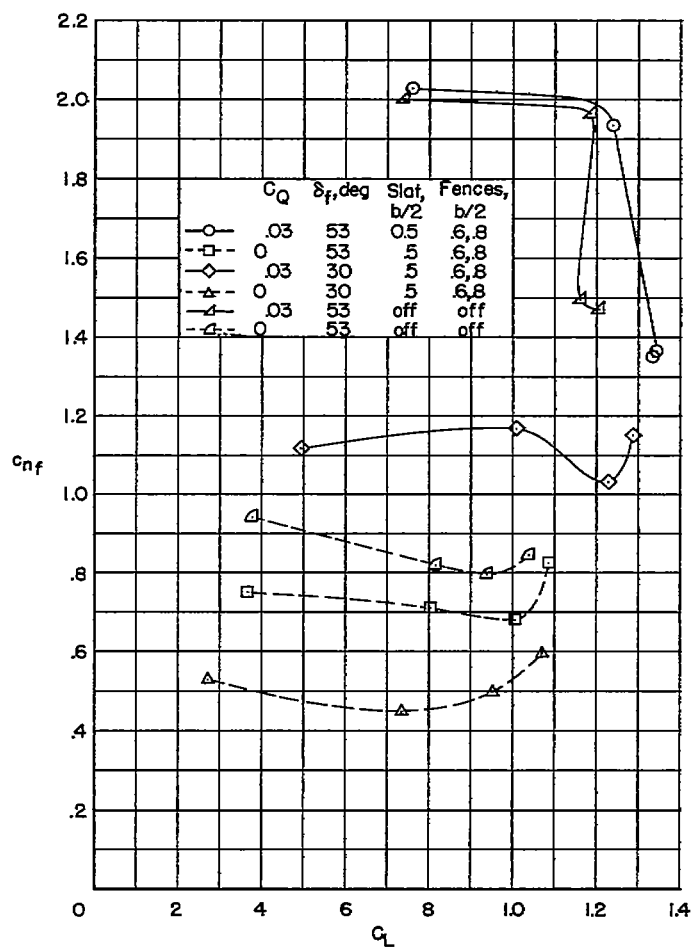
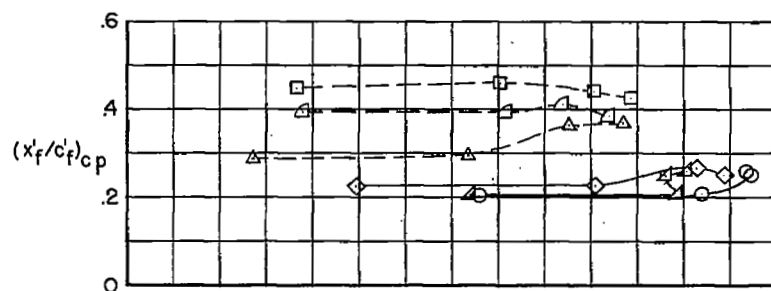
(a)  $c_{c_f}$  against  $C_L$ .(b)  $c_{n_f}$  against  $C_L$ .

Figure 15.- The effect of blowing air over the flap, of flap deflection, and of a slat and fences on flap section coefficients.  $\delta_a = 0^\circ$ ;  
 $R = 4.4 \times 10^6$ .

(c)  $(x'_f/c'_f)_{cp}$  against  $C_L$ .

	$C_Q$	$\delta_f$ , deg	Slot, b/2	Fences, b/2
—○—	.03	53	0.5	.6, 8
—□—	0	53	.5	.6, 8
—◇—	.03	30	.5	.6, 8
—△—	0	30	.5	.6, 8
—▲—	.03	53	off	off
—△—	0	53	off	off

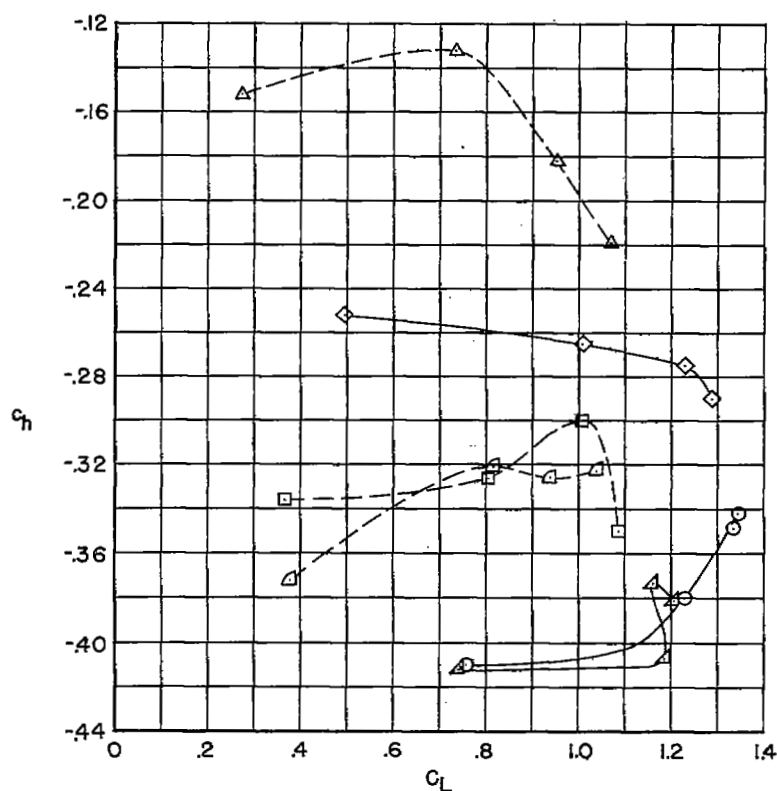
(d)  $c_h$  against  $C_L$ .

Figure 15.- Concluded.

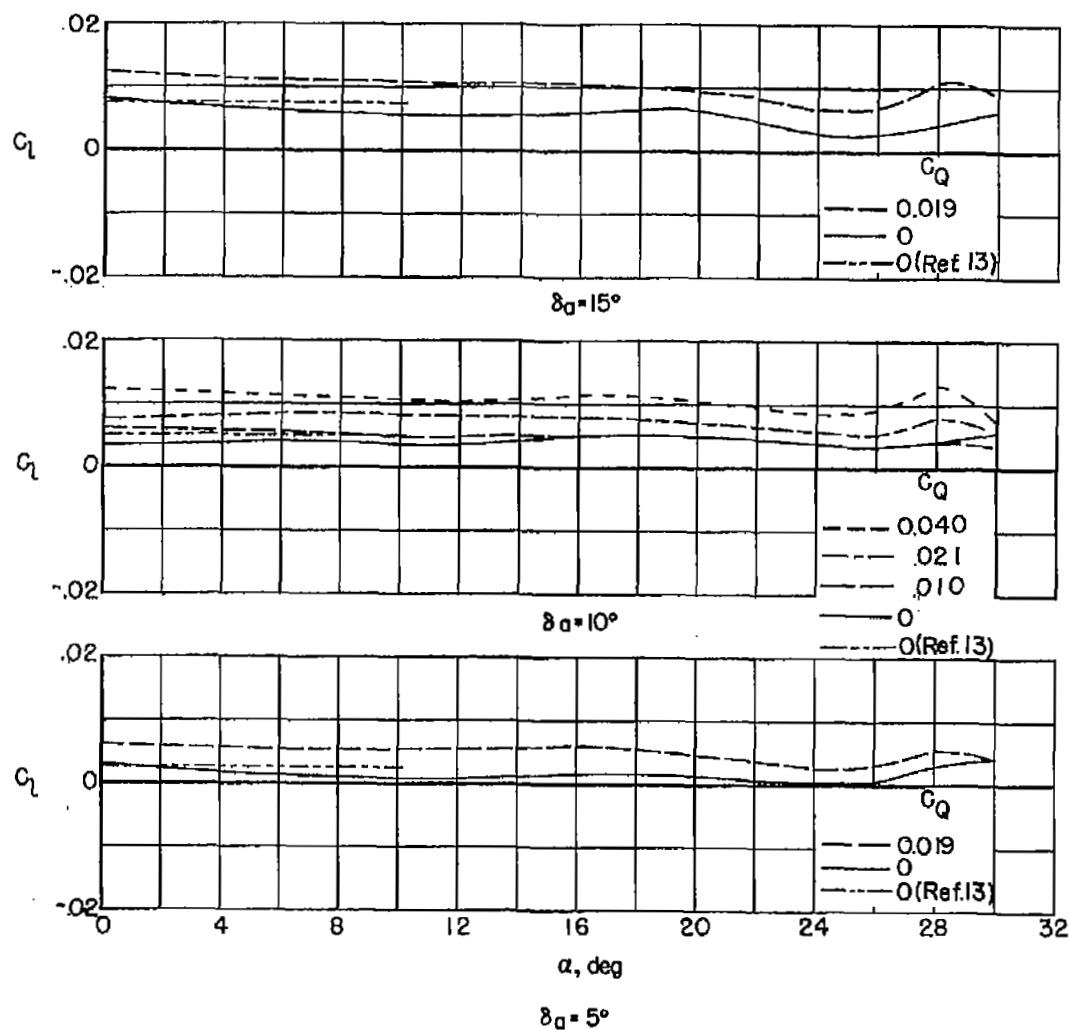
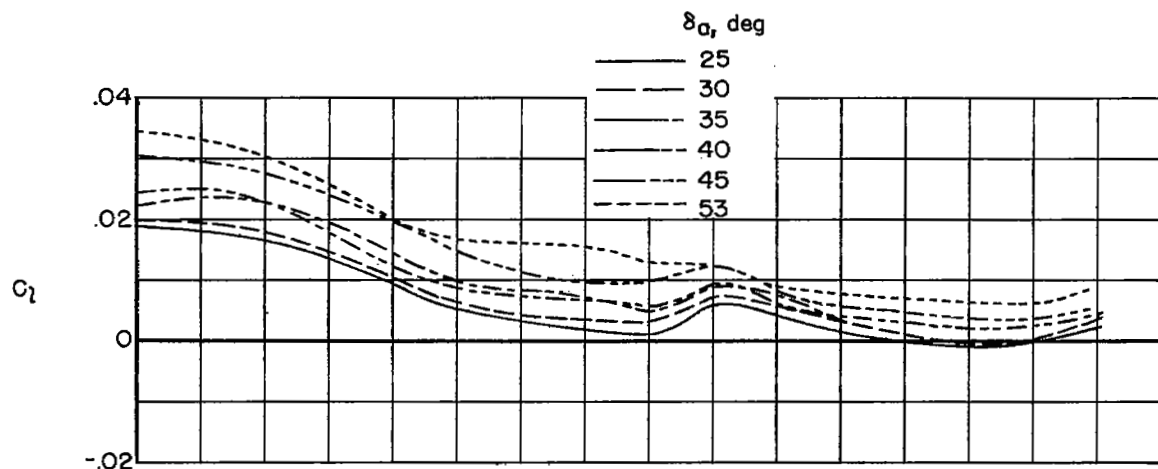
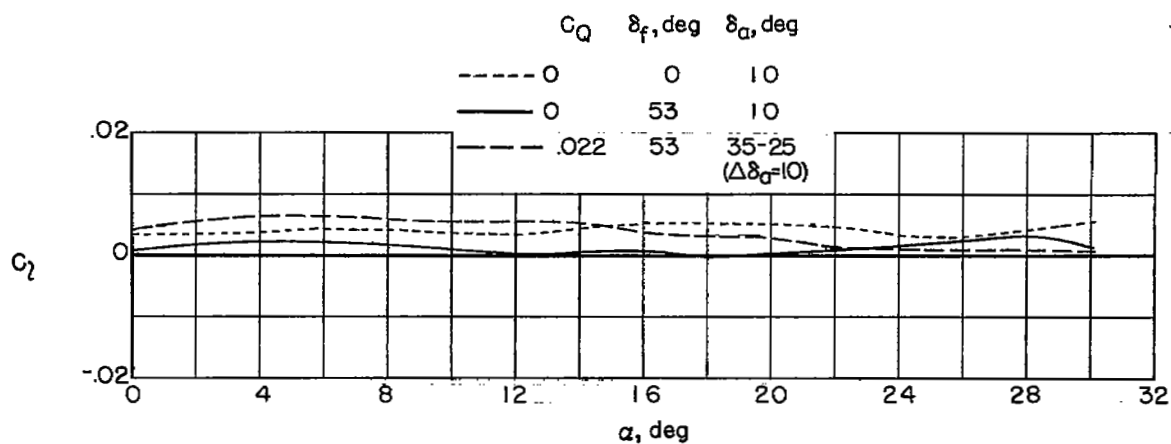


Figure 16.- Effect on the rolling-moment coefficient of the semispan  $49.1^\circ$  sweptback wing of angle of attack, aileron deflection, and  $C_Q$ .  
 $\delta_F = 0^\circ$ ;  $0.5b/2$  slat;  $0.6b/2$  and  $0.8b/2$  fences;  $R = 4.4 \times 10^6$ .



(a) Effect of aileron deflection.  $\delta_f = 53^\circ$ ;  $C_Q \approx 0.02$ .



(b) Effect of flap deflection and  $C_Q$ .

Figure 17.- Effect on the rolling-moment coefficient of the semispan  $49.1^\circ$  sweptback wing of angle of attack, aileron deflection, flap deflection, and  $C_Q$ .  $0.5b/2$  slat;  $0.6b/2$  and  $0.8b/2$  fences;  $R = 4.4 \times 10^6$ . Blowing over the flap and aileron.

	$\Delta\delta_a$	$\delta_f$	$C_Q$
————	0-15	0	0
— · — · —	0-15	0	0.020
— · — · —	25-53	53	0.022
-----	—	0	0 (theory of reference 13)

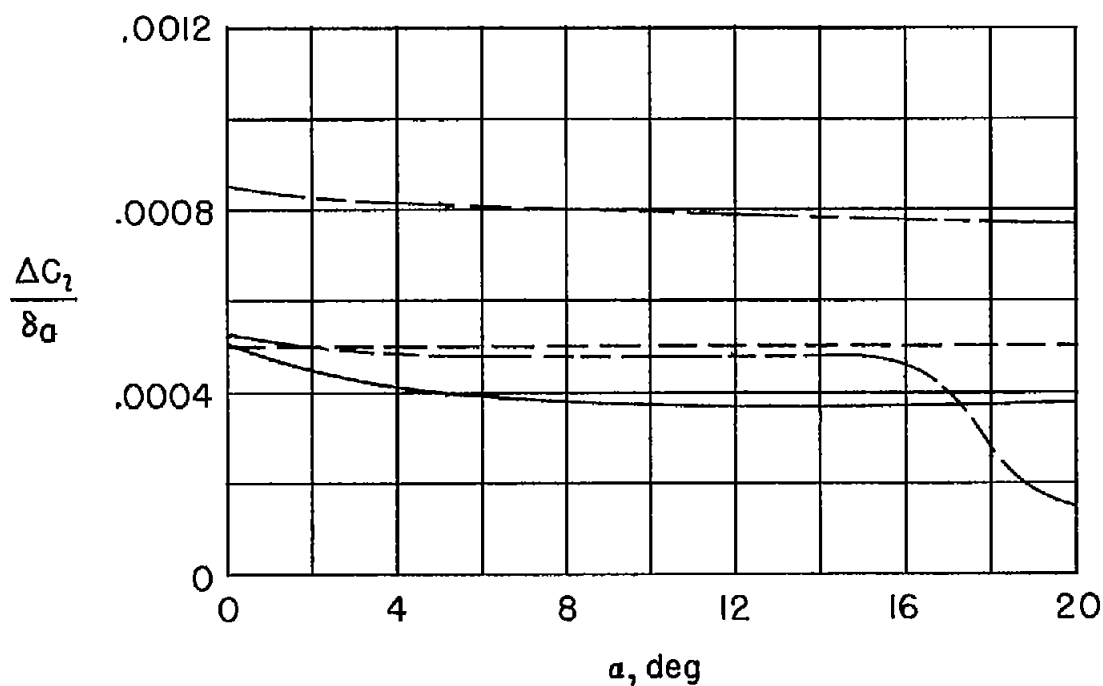
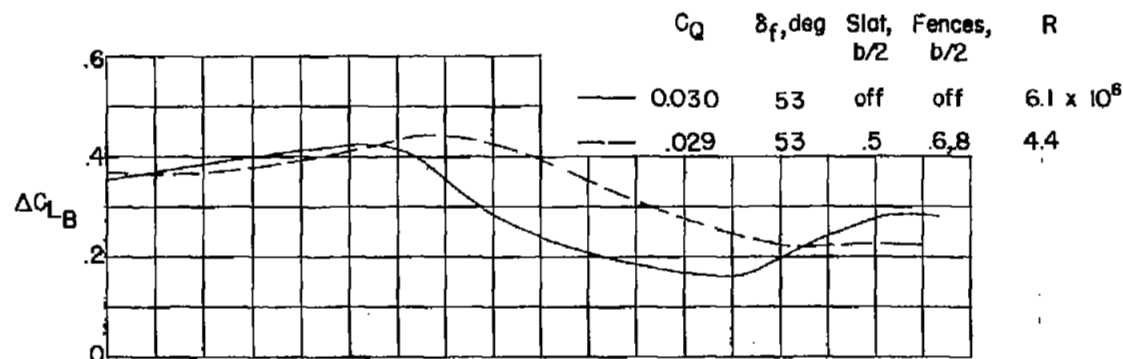


Figure 18.- Aileron effectiveness without and with blowing.





(a) Effect of slat and fences.

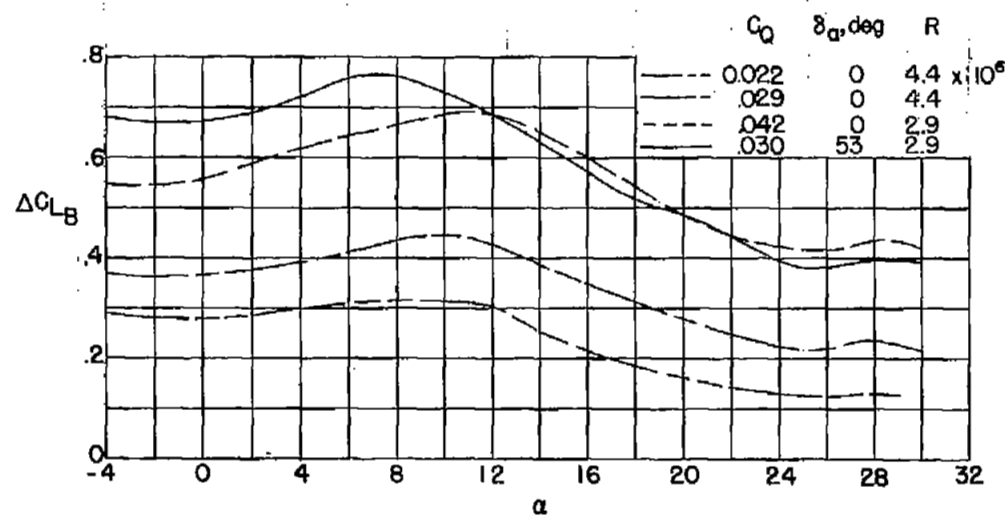
(b) Effect of  $C_Q$ . 0.5b/2 slat; 0.6b/2 and 0.8b/2 fences;  $\delta_f = 53^\circ$ .

Figure 19.- The lift increment due to blowing air over the flap or aileron and flap.

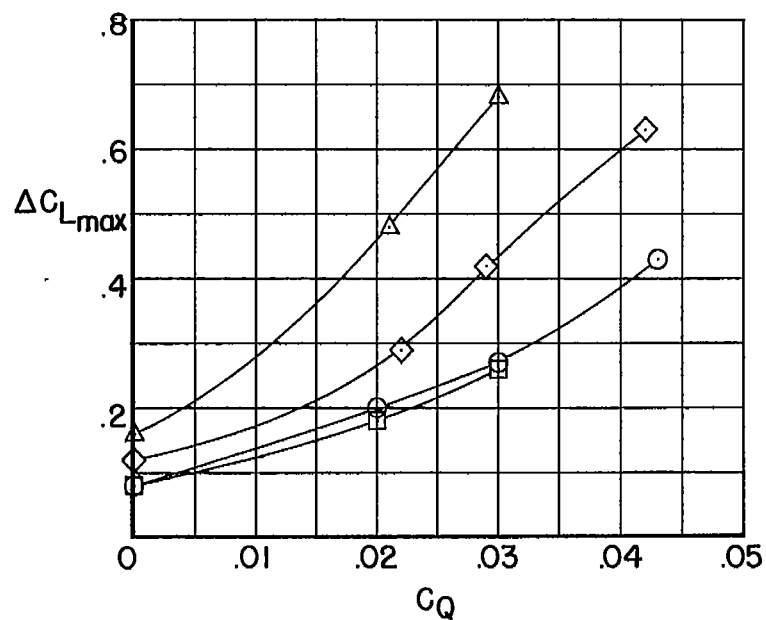
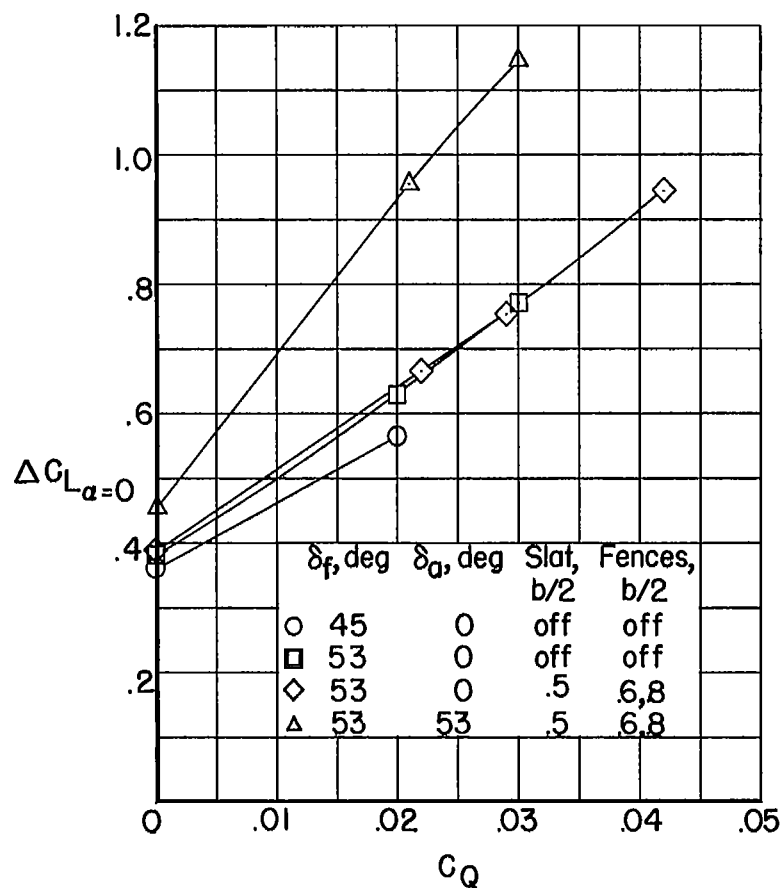


Figure 20.- Summary of the effect on  $\Delta C_{L_{\alpha=0}}$  and  $\Delta C_{L_{max}}$  of  $C_Q$ , flap deflection, aileron deflection, a slat, and fences.

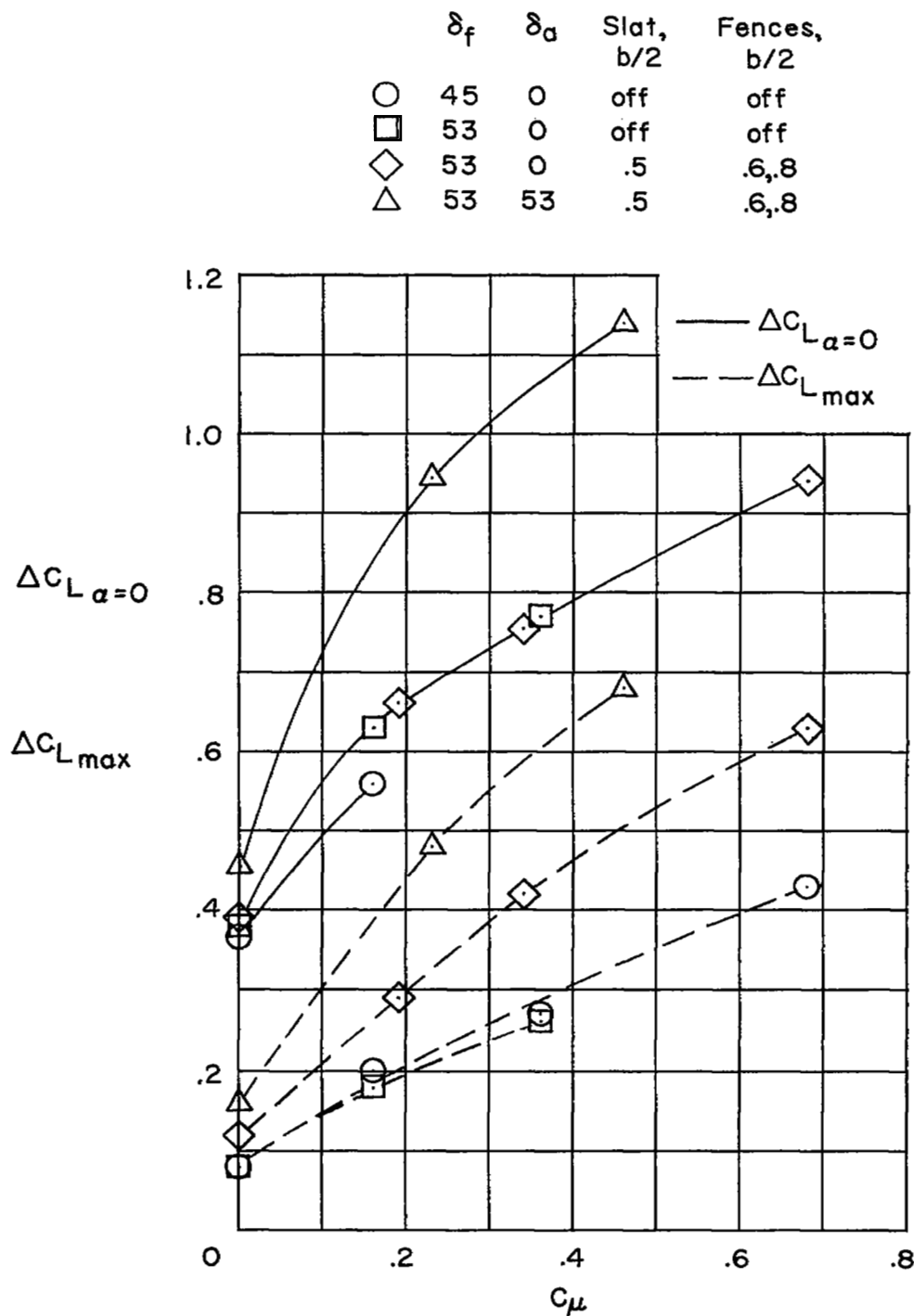


Figure 21.- Summary of the effect on  $\Delta C_{L_{\alpha=0}}$  and  $\Delta C_{L_{max}}$  of momentum coefficient, flap deflection, aileron deflection, and a slat and fences.

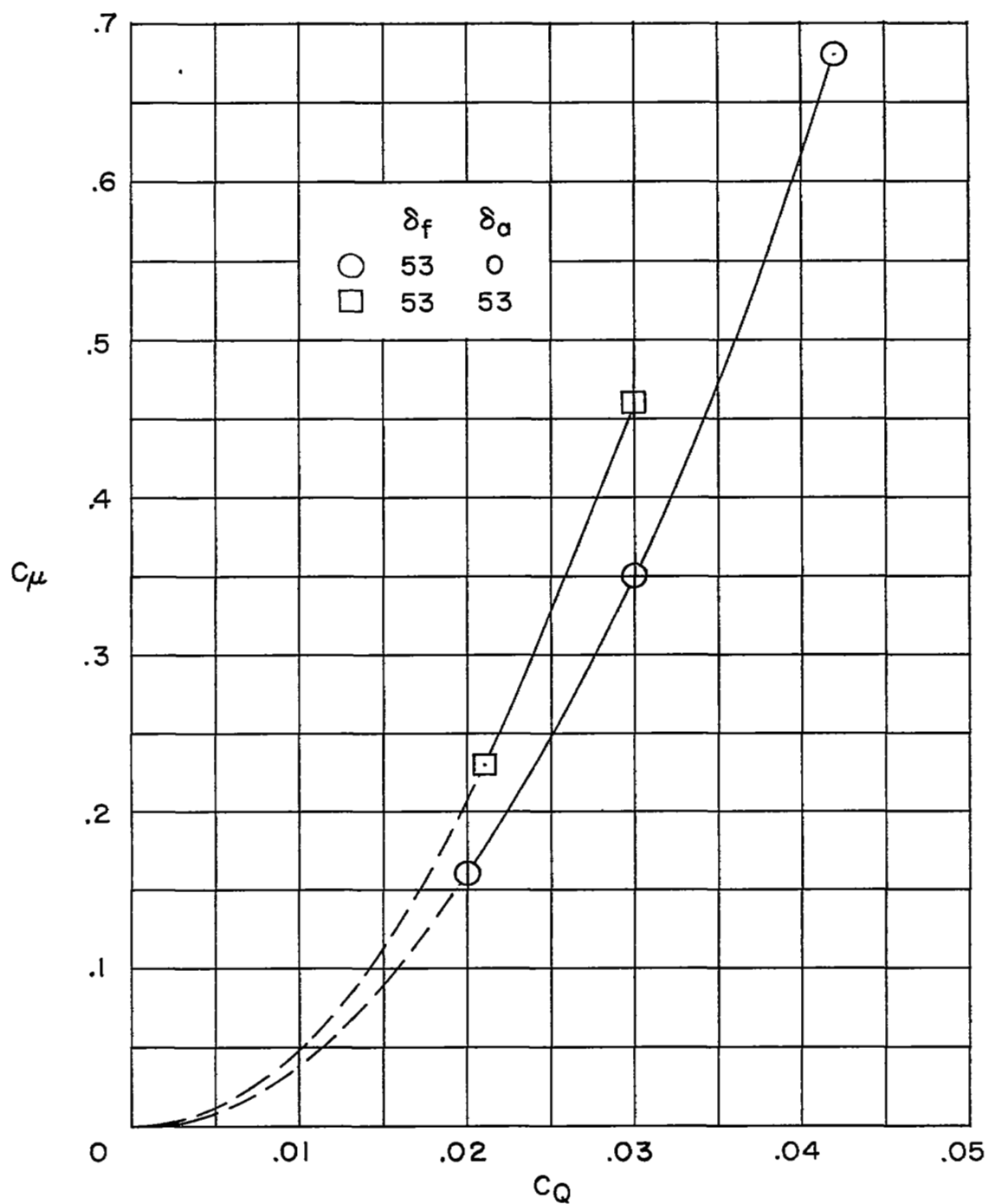


Figure 22.- Variation of the momentum coefficient with the quantity of flow coefficient.

NASA Technical Library



3 1176 01437 1380